REFLECT DELIVERABLE D3.4

OPERATIONAL RISK MAP -

UNCERTAINTIES AND VARIATIONS IN FLUID DATA, IMPROVED RISK MAP WORKFLOW AND CALCITE SCALING RISK MAPS.

Summary:

Risk maps are created with the objective of providing improved operational advice on scaling mitigation. The issue of prevailing uncertainties and variations in fluid and gas data had to be tackled to provide accurate model predictions and risk assessments. The developed risk map workflow is demonstrated for calcite scaling risks of the West-Netherlands Basin.

Authors:

Laura Wasch, TNO, Scientist
Jonah Poort, TNO, Scientist
Marijana Miloshevska, TNO, Scientist
Dorien Dinkelman, TNO, Scientist

This project has received funding from the European Union's Horizon 2020 research and innovation programme under grant agreement nº 850626.

Title:	Operational Risk Map – Uncertainties and variations in fluid data, risk map workflow and calcite scaling risk maps
Lead beneficiary:	TNO
Due date:	31 May 2023
Nature:	Public
Diffusion:	all Partners, EC and general public
Status:	Final
Document code:	REFLECT_D3.4
DOI:	https://doi.org/10.48440/gfz.4.8.2023.008
License information:	CC-BY-4.0
Recommended citation:	Wasch, L., Poort, J., Miloshevska, M., Dinkelman, D., The H2020 REFLECT project: Deliverable *3.4* -Operational Risk Map – Uncertainties and variations in fluid data, risk map workflow and calcite scaling risk map*., GFZ German research Centre for geosciences,* DOI :https://doi.org/10.48440/gfz.4.8.2023.008

Revision history	Author	Delivery date	Summary of changes and comments
Version 01	LW	16.05.2023	Draft
Version 02	JG	17.05.2023	Reviewed
Final version	LW	22.05.2023	Final

Approval status				
	Name	Function	Date	Signature
Deliverable responsible	Laura Wasch	Scientist		
WP leader				
Reviewer	Jasper Griffioen	Scientist		
Reviewer	Katrin Kieling	Project Manager	31 May 2023	
Project Coordinator				

TABLE OF CONTENTS

FIGURES

TABLES

1 EXECUTIVE SUMMARY

The behaviour and composition of fluids and the interaction with the engineered components of a power plant are aspects that influence the efficiency of geothermal energy. One of the main technical issues related to fluid interaction is the deposition of solids on the surface of wells, pipes and heat exchangers. This process of mineral scaling may in time significantly reduce flow and heat transfer and geothermal energy production at large.

REFLECT aims to prevent problems related to fluid chemistry rather than treat them, which requires detailed knowledge on the chemical processes and fluid compositions. Chemical fluid properties are often poorly defined, since sampling and measurement of geothermal fluids are challenging due to the high temperature, elevated pressure and the high concentrations of natural gasses in the fluid. Therefore, large uncertainties in current model predictions prevail, which will be tackled in REFLECT by collecting new data in a web-based repository 'Fluid Atlas' and by tool development for improved predictive modelling and uncertainty quantification. As a final step of the project, these results have been combined with existing temperature maps of the subsurface (ThermoGIS) to create a risk map. The main objective of the risk map is to enable risk assessment of mineral scaling on a regional scale, which provides operators with recommendations on how to best operate their geothermal systems for scaling prevention.

This report describes the developed workflow to create risk maps and contains a demonstration case of calcite scaling in geothermal plants in the West-Netherlands Basin. For low-enthalpy geothermal systems calcite scaling can be controlled by adjusting the top-side pressure in the gas separator tank. Advise on the right pressure enables the operator to prevent harmful carbonate scale deposits, following the basic process of pressure decrease → CO_2 release → pH increase → calcite scaling. Although the issue of calcite scaling is well known from both the geothermal and the oil and gas industry, the uncertainties in fluid composition complicate accurate predictions.

Assessment of uncertainties and natural variations in fluid composition is key in achieving accurate model results, but also gives important insights in the limitations of model predictions. The developed risk map model workflow provides an effective way to tackle some of these limitations. The workflow is especially powerful in evading the significant uncertainties that exist in the measured pH and CO_2 partial pressure of geothermal fluids. These parameters are crucial since they control calcite scaling to a considerable extent. A new approach is proposed that can include uncertainties and variations in these parameters, while still retaining accuracy and precision in model predictions and the derived scaling risk map. Improved recommendations for scaling prevention using the developed model approach are an important step towards better operational practices and enhanced geothermal energy production.

2 INTRODUCTION

The performance of geothermal systems needs to be improved to drive the growth of geothermal energy utilization and support the energy transition. Several operational issues in geothermal energy still need to be solved (Schreiber et al, 2016). A key operational challenge of geothermal energy production is to predict and prevent scale deposition. Scale may deposit when the chemical equilibrium of a fluid is disturbed due to pressure changes during production and resulting gas release (Figure 2.1 point A and B) and temperature changes due to heat extraction (Figure 2.1 point C). Depending on the fluid composition and geothermal conditions a variety of scales may occur including carbonates, silicates, sulphates and metal sulphide precipitates (Todd & Bluemle, 2022). To improve our understanding, predictions and mitigation strategies of scale deposition, it is crucial to have high quality data on fluid compositions as collected in the Fluid Atlas of the REFLECT project (Deliverable 3.3, Kovács et al., 2023).

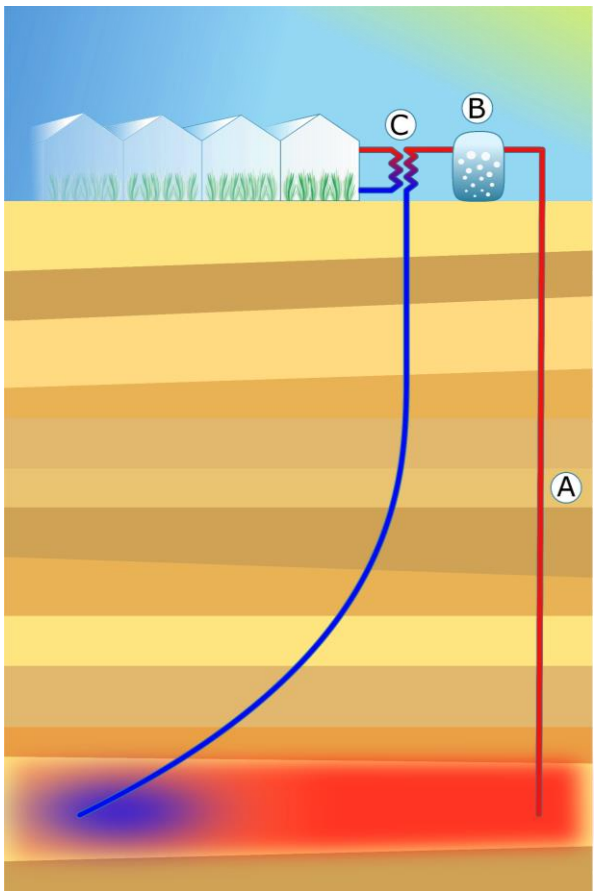

Figure 2.1: Geothermal doublet with A) production well, B) oil and gas separator tank, C) heat exchanger and the reinjection well.

The performance of geothermal plants can be improved by prior information on scaling risks, facilitating the application of appropriate counter measures during the geothermal plant design phase. This will help a more active instead of reactive management of scaling, solving the problems before they occur. A risk map is ideally suited to provide such information on a regional scale, moving from site specific models to a regional assessment of scaling risk based on the pressure and temperature variation.

Two different approaches are presented that may help in determining scaling risks on a basin to European scale. The first approach included principal component analysis on all data collected in the Fluid Atlas and the second approach is the development of regional scaling risk maps. The first tool can be used to find sites with similar fluid compositions to learn from their experiences and identify expected scale minerals. The fluid/gas composition of a well's brine can provide insights into potential operational (scaling) risks of the well in question. In addition, by comparing the brine of one well to that of others it is possible to assess how similar they are in brine composition. This information could then be used to anticipate on operational issues by linking wells with known issues to those with similar brines. The second

approach is the risk map, which provides an assessment of the quantitative scaling risk for one scale mineral. A specific case is selected for the risk map. Prior to creating the risk map, a detailed assessment of the uncertainties and variations of the selected case is performed.

To create a risk map sufficient good quality data and robust models must be in place. Several options were explored for a demonstration case. Two cases were considered related to the model development in WP4: scaling in the geothermal wells of the Tuzla region and barite scaling in the Netherlands (Deliverable 4.2 and 4.3). The models developed for the Tuzla region proved difficult to match to the data, while the scaling behaviour is very complex with multiple minerals and chemical processes. The barite scaling case has robust models, however there is no known data on occurrences of barite scaling in the Dutch sites, making the risk assessment difficult. Finally, a third option of calcite scaling in the Netherlands was chosen since a lot of data was available in the Fluid Atlas and there are known occurrences of carbonate scaling (Wasch et al., 2022).

2.1 SELECTED SITE: WEST NETHERLANDS BASIN

The selected doublets are located in the West Netherlands Basin. This area is the Netherlands' most exploited geothermal reservoir with 20 doublets drilled in 18 different sites since the first geothermal well drilled in 2007 (www.nlog.nl). The wells produce from Jurassic and Cretaceous reservoirs with temperatures between 60 and 100 °C and depths between 1.5 and 3 km (Figure 2.2). Of these wells, eight wells/sites are selected that have a good quality and complete set of fluid and gas data (Table 1). The main target of these wells is the Delft Sandstone Member (SL) with additional production from the Alblasserdam Member (SL), Berkel Sandstone Member (KN) and Rijswijk Sandstone Member (KN). The temperature of reservoirs is below 100°C and is considered 'low enthalpy'. The produced water is used for heating greenhouses, buildings and swimming pools.

Table 1: Overview selected geothermal sites (www.nlog.nl)

Site	Well	T (°C)	P (bar)
De Lier	LIR-GT-01	88	242
Maasland	MLD-GT-01-S1	94	280
Brielle	BRI-GT-01	80	206
Lansingerland	LSL-GT-01	61	160
Den Haag	HAG-GT-02	76	206
Honselersdijk	HON-GT-01	84	274
Poeldijk	PLD-GT-01	86	250
Pijnacker	PNA-GT-05	76.5	200

The West Netherlands Basin is a transtensional basin composed of structural highs and lows with a NW-SE orientation, formed by rifting occurring from the Late Jurassic to the Early Cretaceous (Van Balen et al., 1999). The syntectonic deposition comprises mainly fluvial deposits. When rifting slowed, basin subsidence resulted in marine transgression and a transition to a marine depositional environment. A later phase of compressions in the Late Cretaceous caused inversion, uplift and erosion, and fault reactivation (Donselaar et al. 2015, Van Balen et al. 1999). The composition of the sandstone reservoir rocks is quartz dominated with kaolinite (1-7%), other clays (1-13%), siderite (<4%), varying amounts of calcite (0.3 to 40%) and minor pyrite, hematite, rutile and chlorite (Wasch et al., 2020).

The West Netherlands basin is well known for its hydrocarbon charging and oil and gas fields. Even when no hydrocarbon traps are present, the migration of hydrocarbons result in oil, gas and CO_2 dissolution in the aqueous fluid of the geothermal reservoirs. Considerable amounts of natural gas can be produced with the geothermal water as the gas (and oil) come out of solution with pressure decrease. The geothermal plants often have an oil and gas separator tank to produce the gas and separate it from the fluid that is reinjected. Several of the sites use the methane as an additional energy source but methane combustion also releases greenhouse gasses into the atmosphere.

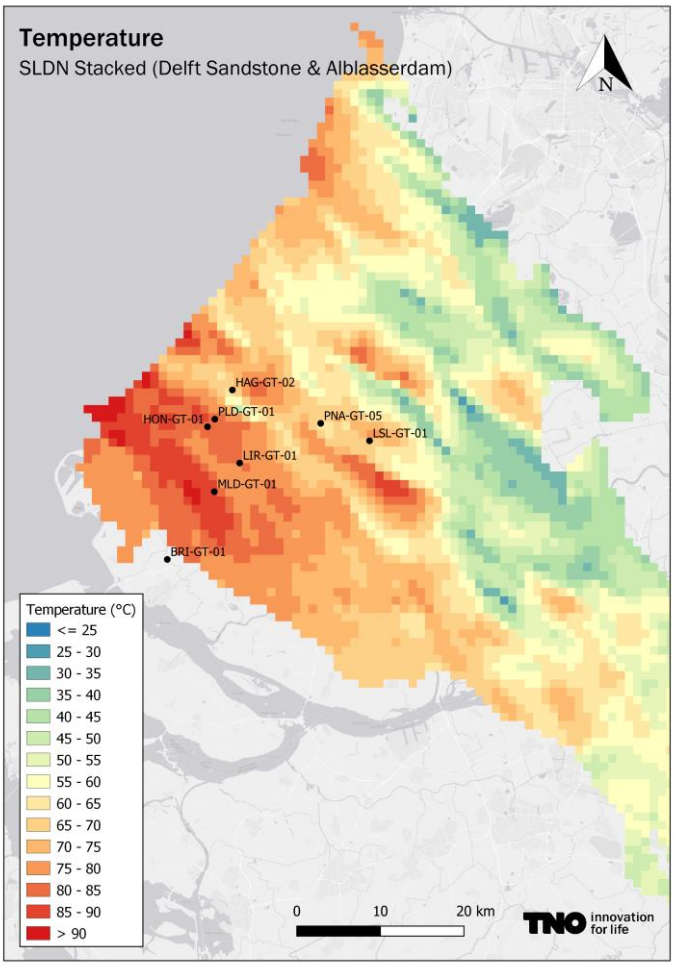

Figure 2.2: Temperature map (www.thermogis.nl) with the selected sites.

2.2 SELECTED RISK: CALCITE SCALING

Carbonate scaling is a common issue for low-enthalpy geothermal systems (Schreiber et al., 2016). In the case of geothermal energy, the precipitation of carbonates is caused by (partial) outgassing of the geothermal fluid during production. The solubility of gasses decreases with lower pressures, and the naturally dissolved gasses escape the fluid. For the West Netherlands Basin, the dissolved gasses consist mainly of CH_4 (methane) and CO_2 (carbon dioxide). The release of CO_2 has a large impact on water chemistry, since it causes a pH rise (equation 1-2) which can cause calcite precipitation (equation 3-4).

$$CO_2 + H_2O \leftrightarrow H_2CO_3 \quad [1]$$
$$H_2CO_3 \leftrightarrow H^+ + HCO_3^- \quad [2]$$
$$HCO_3^- \leftrightarrow H^+ + CO_3^{2-} \quad [3]$$
$$CO_3^{2-} + Ca^{2+} \leftrightarrow CaCO_3 \quad [4]$$

By maintaining a higher operational pressure in the geothermal installation, sufficient CO_2 is kept in solution to keep the pH sufficiently low to prevent carbonate scaling (e.g. Wasch et al., 2022). Finding the required pressure to prevent calcite scaling is the base for operational advice by the performed predictive modelling and risk mapping.

2.3 DEFENITION OF SCALING RISK

We define the scaling tendency by the mineral supersaturation which is indicated by the saturation index. Geochemical modelling software such as PHREEQC calculates the saturation index (SI) of minerals for a specific fluid composition, and pressure and temperature (Parkhurst and Appelo, 2013). The saturation index is calculated by comparing the chemical activities of the dissolved ions of the mineral (ion activity product, IAP) with their solubility product (Ksp), equation 5. With supersaturation (tendency to precipitate) indicated by a positive saturation index and undersaturation (tendency to dissolve) indicated by a negative saturation index. Equilibrium between minerals and the fluid is indicated by a SI of 0.

$$SI = \log\left[\frac{IAP}{K_{sp}}\right] \quad [5]$$

With the assumption of calcite saturation at reservoir conditions, calcite becomes supersaturated with pressure decrease and associated degassing in the production well. Considering the surface pressures between 3 and 10 bar of Delft doublets, we know that a significant pressure drop does not yield scaling in the wellbore. For the Pijnacker site, the pressure can be decreased down to 4 bar – with significant CO_2 outgassing – and no scaling occurs (Wasch et al., 2022). Only increased outgassing and pH rise at a 2 bar pressure will lead to carbonate precipitation. This indicates that a significant supersaturation is required before calcite nucleates and crystal growth occurs.

The required supersaturation is related to a kinetic limitation on calcite precipitation which is most pronounced for low temperatures. The kinetic limitation affects both the first step of

nucleation (when no carbonates are present) and the second step of crystal growth. The complex behaviour of calcite precipitation can be modelled specifically (Lassin et al. 2018). By using a specific supersaturation as a calcite scaling threshold, all the processes are included implicitly. The supersaturation threshold above which scaling occurs is defined as the critical saturation index.

The scaling risk can be defined by how much a modelled saturation index exceeds a critical saturation index. The models for the West Netherlands will be used to define which saturation index (which supersaturation) represents a high risk of scaling. For our case, the critical saturation index will be based on the experiences with calcite scaling at the Pijnacker site. The operators observed carbonate scale deposition when the top side pressure in the plant was set at 2 bar. The modelled supersaturation at these operational conditions will be considered a serious scaling risk. For the risk map, the mapped supersaturations will be compared to this value for the critical saturation index.

3 METHODOLOGY

In this chapter the methods and approaches used to investigate scaling risks are discussed.

3.1 DATA ANALYSES

The fluid/gas composition of a well's brine can provide insights into potential operational (scaling) risks of the well in question. In addition, by comparing the brine of one well to that of others it is possible to map wells not only on their geographical location, but also on how similar they are in brine composition. This information could then be used to anticipate on operational issues by linking wells with known issues to those with similar brines. In this work package, a first step was made in the development of such a tool. Principal component analysis (PCA) was used to reduce the often high-dimensional brine composition in order to make it possible to visualize and compare them in a simple way. In addition, uncertainty quantification (see also Section 3.3) was used to include uncertainty in the measured brine when making the comparison.

The next subsection gives a brief overview of the PCA method and how it was used to compare brine compositions, while chapter 4 gives the results of the PCA method applied to the data in the fluid sample database created in the REFLECT project.

3.1.1 Principle component analysis

Principal component analysis (PCA) is a dimension-reduction technique (Brunton & Kutz, 2017), which is typically used to decrease the dimensionality of a dataset in order to make it easier to visualize, interpret, process, model, or group. For instance, when a dataset contains more than three variables (in reality, most datasets contain far more than three variables), it is no longer possible to plot the data in an easy to interpret manner. In this case, PCA can reduce this data back to a more manageable number of variables while still maintaining the majority of the information in the dataset.

PCA is a linear transformation that maps high-dimensional data to a lower dimensional representation (coordinate system) while preserving as much of the information (variance) of the data in the lower dimensions (Brunton & Kutz, 2017). This transformation is expressed as a number of principal components, a set of orthogonal vectors that best fit the higher-dimensional data. The first principal component is the vector that best fits the higher dimensional data, the second principal component is the next vector that best fits the higher dimensional data that is also orthogonal (right-angled) to the other principal component, etc. See Figure 3.1 for a visualization of this concept.

Using the principal components the original high-dimensional data can be transformed to the new lower dimensional dataset, and can, since the principal components are orthogonal, easily be plotted on a reduced coordinate system. In addition, since PCA makes use of the correlations between variables in the original data to construct the principal components, datapoints that are highly correlated in the high-dimension data will remain highly correlated in the reduced dimension. Thus similar datapoints in a PCA plot, will also be similar in the

original dataset. This fact can be used to more easily compare and group brine compositions in a single two-dimensional PCA plot than based on the original composition data.

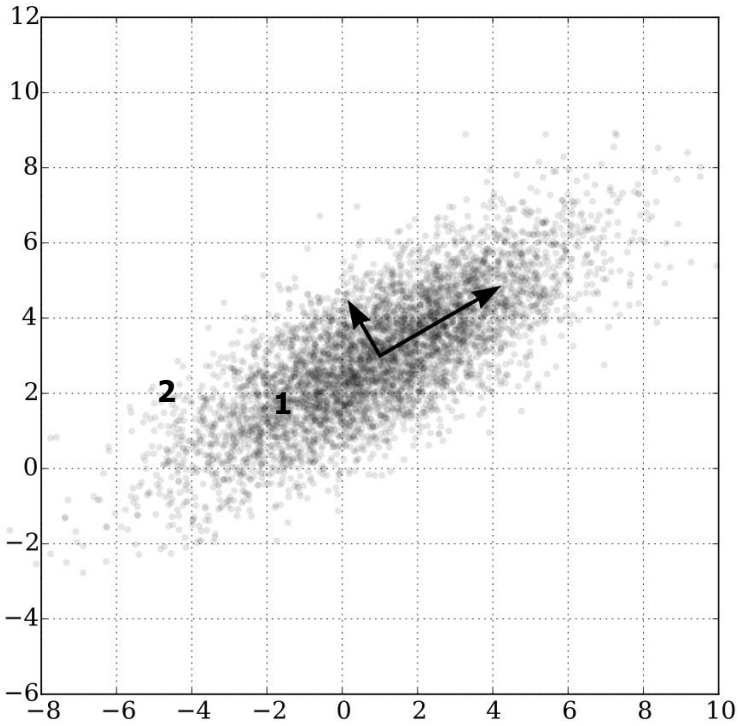

Figure 3.1: Visualization of the first two principal components on a Gaussian dataset. The first principal component is in the direction of the best fit on the data, while the second principal component is in the direction of the next best fit on the data while at the same time being orthogonal (right-angled) to the first principal component.

3.2 GEOCHEMICAL SIMULATOR

The software PHREEQC is used to simulate the scaling potential of the geothermal brine due to temperature and pressure changes in the geothermal installation. PHREEQC version 3 is a computer program designed to perform a wide variety of aqueous geochemical calculations (Parkhurst & Appelo, 2013). Several thermodynamic databases are available for PHREEQC, which include the solubility constants of a set of minerals and gasses at a range of conditions. For this study we selected the Pitzer database (downloaded with PHREEQC v3) which is suitable for calculations of mineral and gas solubility at high salinity.

3.3 UNCERTAINTY QUANTIFICATION

Operational risks such as scaling are largely affected by a geothermal system's brine composition and its operating conditions (e.g. pressures and temperatures in the system). However, the exact brine composition is often unknown, as measurements come with a given uncertainty. As a result, the brine composition, and therefore the associated scaling potential, is never known precisely.

By using the geochemical model, the uncertainty in scaling potential can be evaluated using uncertainty quantification methods. In short, such methods randomly vary a given nominal brine composition and use the geochemical model to calculate the saturation indices of compounds of interest. By performing a large number of such calculations with randomly sampled brine composition, statistical analyses can be performed on the resulting saturation indices to evaluate the impact of brine uncertainty on scaling risks.

Except for some minor changes, the uncertainty quantification method used in this work package is the same as the method developed in work package 4. Therefore, the reader is referred to Chapter 4 for details on the exact methods, (specifically Sections 4.2.1 and 4.2.2) of deliverable D4.2 of the REFLECT project (Poort, de Zwart, Wasch, & Shoeibi Omrani, 2022).

For the purpose of this analysis, the uncertainty quantification tool was updated and used in order to predict the calcite saturation index. The uncertainty analysis can be performed by defining the nominal values of the pH and partial pressure of CO_2 to be varied within a specified range. By using the variation in fluid and CO_2 content, the geochemical model is run for a set of brine compositions. Since the model produces a very large range in calcite saturation indices, the prediction of scaling risk is made more precise by filtering the output data, such that the calcite SI satisfies only a specific range of values (SI = 0). By doing this, a function dependent on pH and CO_2 partial pressure can be obtained, such that it satisfies the SI range of values. The functionality of the uncertainty analysis is explained in further detail in section 6.

4 ANALYSES OF UNCERTAINTIES AND VARIATIONS IN THE EUROPEAN FLUID ATLAS USING PCA

In this chapter, the results of the PCA data analysis applied to the REFLECT fluid database is discussed. The first section will briefly describe what data is found in the database, and what data was used for the analysis, the second section provides the results of the PCA analysis.

4.1 THE FLUID SAMPLE DATABASE

The REFLECT fluid sample database created for the Fluid Atlas is a large excel sheet containing the results of liquid (and sometimes gas) composition measurements of brine samples taking at sites all across Europe. The database contains measurements for over 3500 samples taken at around 1400 unique sites. For each sample, the concentrations of major cations (Ca, Mg, Na, K) and anions (Cl, S, F, CO_3, HCO_3, SO_4, PO_4) are reported. In some cases, also the concentrations of dissolved silica, trace elements (e.g. Ba, Fe, Pb, Sr, Zn), and/or gases (e.g. CO_2, O_2, CH_4, N_2) are listed. In addition, general information such as sampling depth, sampling date, sampling method, are also given when available.

Due to the fact that the samples in the database all come from widely differing origins, with measurements being done for a range of goals, the variables reported can vary considerably from one sample to another. As a result, the items that have been analysed are not the same for all samples in the database. For instance, while one sample may contain values for all major cations and a good number of trace elements, it might only report the values for a few major anions, while another sample reports all major cations, anions and dissolved gases, but no trace elements. As a results, it is very difficult to fairly compare all samples in the database.

In order to mitigate this problem, it is possible to define a list of variables (cations, anions, trace elements) of interest, and only include and compare samples from the database that contain measurements for those variables in the analysis. However, the longer this list of variables is, the fewer samples will be present in the database that contain all variables in it. In addition, certain variables might be so rare that almost no sample contains it, and thus the statistical analysis can only be performed on a very small dataset.

To illustrate the issue described above, an analysis was run on the dataset to find the set of elements that result in the largest number of samples that contain measurements for all the elements in the set. To reduce the number of possibilities, the analysis was restricted to 14 variables of interest (Cl, SO_4, Na, Ca, Mg, Sr, K, Mn, Ba, Pb, O_2, N_2, CO_2, CH_4). The analysis was performed for element sets of lengths between 14 and 5. When looking at a set of 6 elements, the method aims to find which combination of 6 elements from the original 14 have the most overlap in measured concentrations across all fluid samples. For instance, there might be around 200 samples that have measurements for all elements in the set Cl, Na, Ba, Pb, CO_2, and CH_4, but there are almost 2300 samples that have measurements for all elements in the set Cl, SO_4, Na, Ca, Mg, and K. Figure 4.1 gives an overview of the combinations of elements that give the highest number of fluid samples for a certain number of variables. As expected, the larger the number of elements, the fewer fluid samples are found that fit the criterion set.

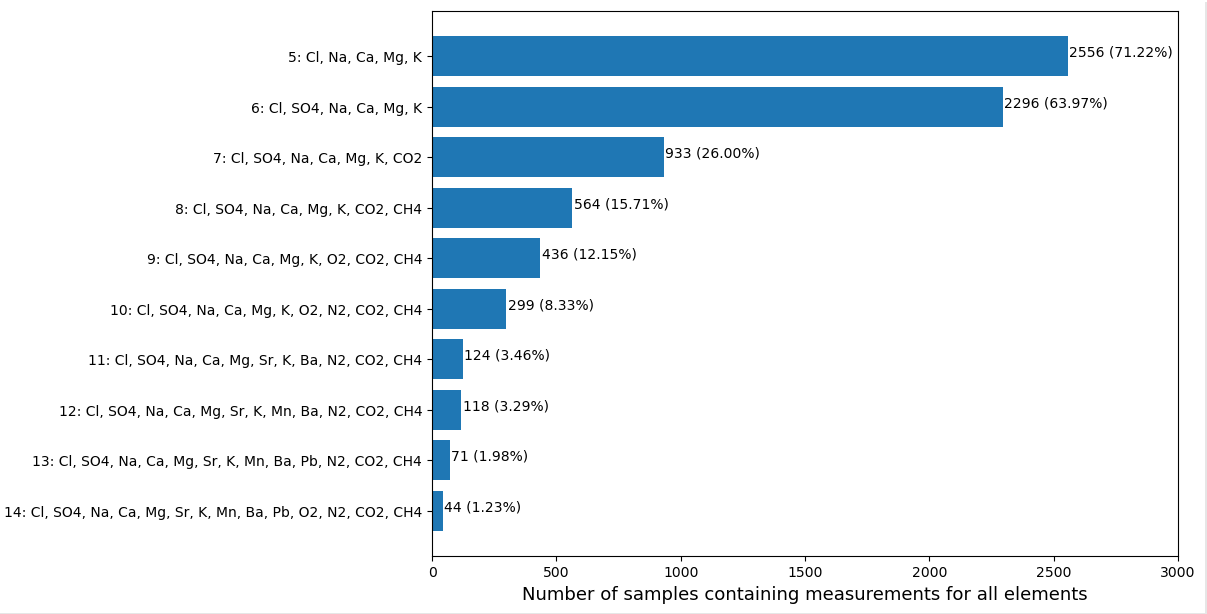

Figure 4.1: Number of fluid samples containing measurements for all elements in the shown list of elements. Reported values are for the combination of elements that result in the highest number of fluid samples for combination lengths between 5-14.

4.2 PCA RESULTS

The previous section showed that when more elements are included in the PCA analysis, the fewer fluid samples can be compared. Therefore, there is a trade-off in how much information of the fluid sample can be used, versus how many samples can be evaluated. More elements will allow for a more comprehensive analysis of the brine similarity, but at the same time will mean fewer samples can actually be compared with each other.

At the same time, it can also be argued that the elements that occur the most in the fluid database do so because they are also those of highest interest (and vice versa, those that are of lesser interest are less often measured). For this reason, this section will report the result of the analysis done for the combination of 6 elements (Cl, SO_4, Na, Ca, Mg, K), as it contains values for all cations and two of the most important major anions.
Figure 4.2 shows a plot of all fluid samples based on the first two principal components coloured by the country of origin. As the figure shows, the samples get divided into groups that stand apart, these are:

1. The largest group of sites with fluid compositions that lie close to the general average of the entire dataset. Sites in this group are present all over Europe, with most wells coming from Greece, Turkey, Hungary, and Iceland.
2. A smaller group with average concentrations calcium, and higher concentrations for chlorine and sodium. Most wells in this group come from France and Belgium, with a few wells from Germany and the Netherlands

3. A widespread group of wells with high chlorine and sodium contents, but low values for calcium. Wells in this group primarily come from the Netherlands, Denmark, and the UK, with a few wells from Germany.
4. A group of wells with high concentrations of chlorine and calcium, and relatively high sodium concentrations. Especially the wells in the top right of the plot have very high calcium contents and come from two specific sites in Germany, while the other wells in this group come from Denmark and one from the UK.

In general, the primary PCA axis corresponds to the chlorine (and to a lesser extend sodium) content, while the secondary PCA axis corresponds to the calcium content. Concentrations of the other ions (K, Mg, SO_4) seem to have much smaller impact on the place of a sample in the plot.

The results of the analysis seem to align quite well with geological proximity of wells, with an interesting result that Icelandic brine is very comparable to that of brine from South-East Europe. This could be due to high volcanic activity in these countries, which could lead to similar brine contents that differ significantly from the countries with lesser geological activity (North-West of mainland Europe).

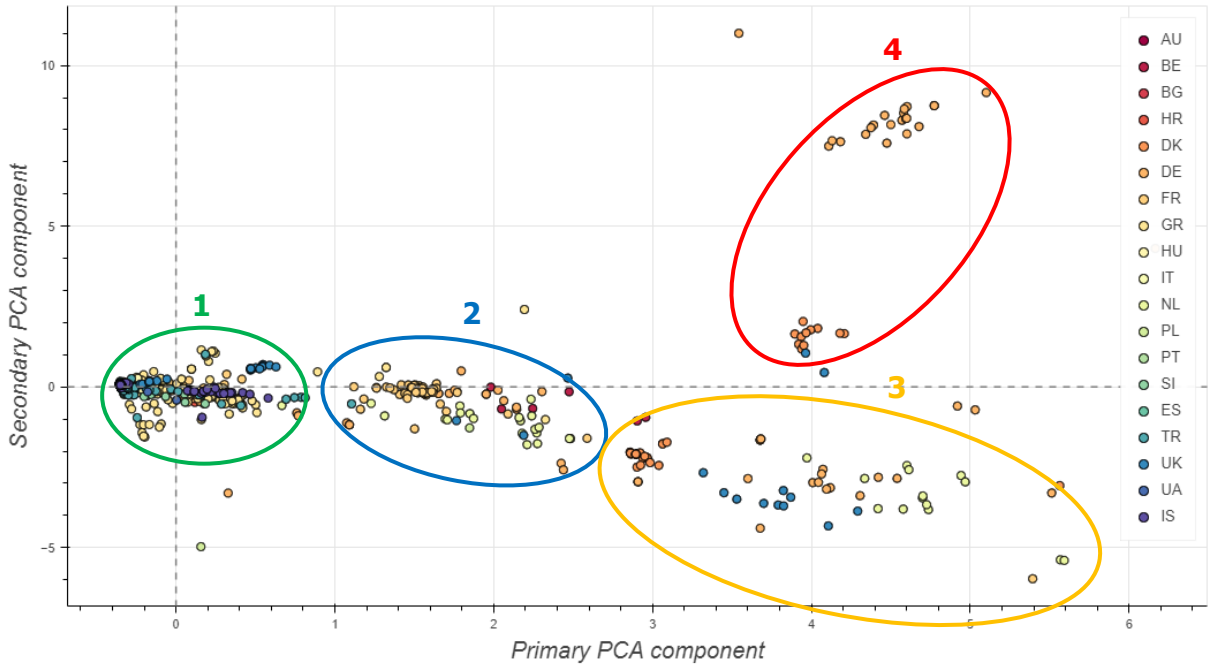

Figure 4.2: Plot of the first two principal components of the REFLECT fluid sample database comparing 2296 samples on Cl, SO_4, Na, Ca, Mg, and K. Colours indicate fluid samples from sites in the same country.

4.3 PCA TOOL

While the analysis from the previous section provides interesting insights into how the wells in the REFLECT project compare based on fluid composition, it covers only a limited number of elements in the analysis. Furthermore, the most useful application of PCA is to compare a specific well to all others in the database to see which ones it most closely resembles in order to anticipate upon operational issues found in literature for such wells.

For this reason, a Python tool/app was developed that allows the user to provide their own brine composition (including uncertainty levels), set whichever combination of elements they are interested in, and automatically perform the analysis on all fluid samples containing measurements for those elements. Results are shown in an interactive plot that allows the user to hover over specific points of interest to see additional information from the database, where available.

The tool/app can be made freely available to all partners within the REFLECT project (it does require some knowledge of Python)[1].

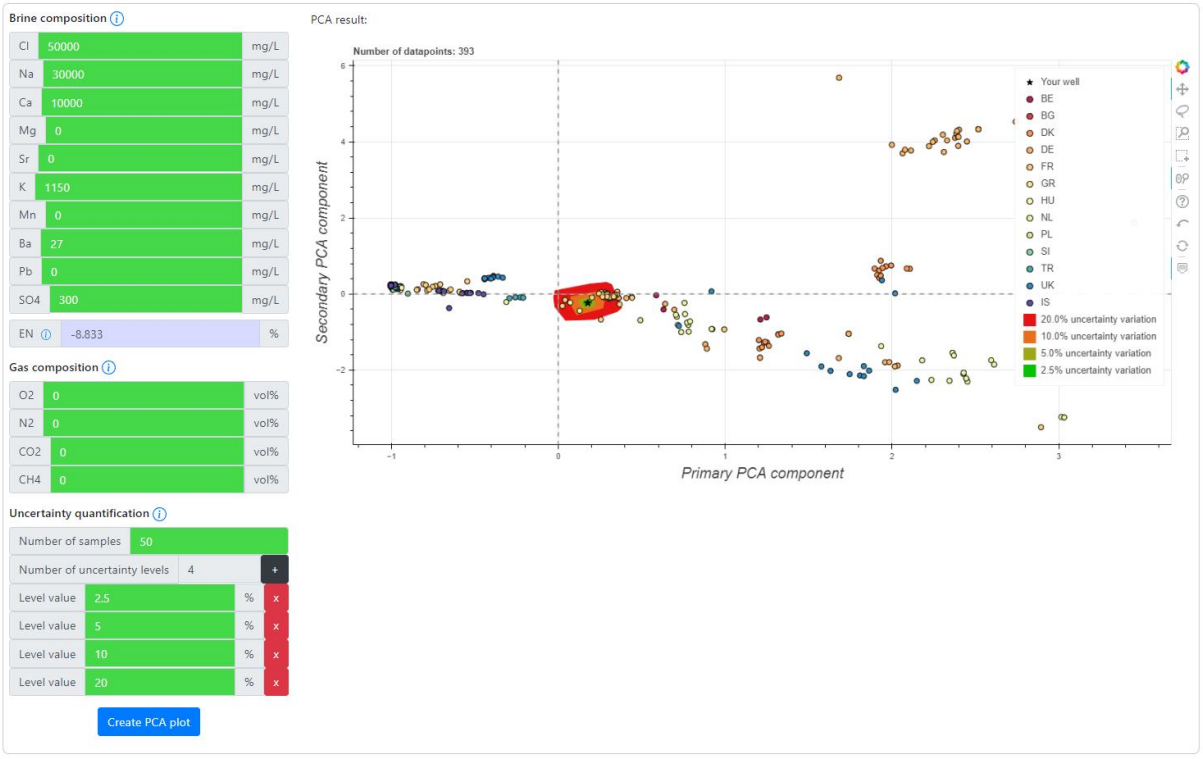

Figure 4.3: Screenshot of the interactive PCA tool.

[1] If interested please contact jonah.poort@tno.nl.

5 UNCERTAINTIES AND VARIATIONS IN FLUID DATA OF THE RISK MAP DEMONSTRATION CASE

Prior to creating the risk map, the uncertainties and variations of the fluid and gas compositions reported for the sites are assessed.

5.1 UNCERTAINTY IN GAS DATA

All the selected doublets produce fluids with dissolved natural gases. There is a variation in both gas composition (Table 2) and fluid composition (Table 3). The gas contains mainly CH_4 with variable amounts of CO_2. On top of the natural variation, the reported data on the total gas pressure and the gas composition can have large uncertainties. This is mainly due to the sensitivity of sampling fluids that outgas with pressure decrease during production. Ideally, the fluid is sampled with a bottom hole sampler to measure the original (one phase) reservoir fluid. Since produced fluids already partially degas before reaching the surface, surface fluid samples are incomplete regarding the gas content or the gas water ratio (GWR).

The effect is clear when pressurized fluid samples are taken at different locations with different pressures. For example, well LIR-GT-01 showed a GWR of up to 0.88 for the bottom hole sample (BHS), a slightly lower GWR of 0.75 at 20.3 bar and a much lower GWR of 0.25 at 8 bar (Table 2). For well MLD-GT01-S1, the GWR is 0.78 for the BHS and 0.22 for the surface sample. The lower amount of gas in the surface fluid samples is reflected in a lower calculated bubble point as well, which is 48.3 for the BHS and 6.6 bar for the surface sample (Table 2). There appears to be a problem with the data of the PLD-GT-01 BHS, as it has very low GWR and bubble point, both lower than for the surface samples. Although a BHS is most ideal, the issue with the PLD data and the imprecise data for De Lier (GWR 0.72 and GWR 0.88) indicate that uncertainties are still considerable.

If no BHS has been collected, the incomplete GWR of a surface sample can be corrected. The water and gas analyses (PVT) report for HAG-GT-02 mentions a calculated GWR of 0.93 for the separator tank and a calculated full GWR of 1.62, while the GWR values for the surface sample are around 0.5. Since the correction was not described in the report and since there are no other records of such a high GWR, the GWR of 1.62 cannot be confirmed with certainty. In the PVT report for HON-GT-01 the issue of incomplete surface GWR measurements is also addressed and the measured values of 0.812 and 0.896 in a surface bypass were corrected to 0.93 and 1.01. This correction is much smaller than the correction reported for HAG-GT-02.

Without or next to a measured or corrected GWR, the production data is often used to assess the GWR and gas composition as this data is available for all geothermal doublets of the Netherlands. To calculate the GWR ratio from production data, the produced mass of gas is simply divided by the produced fluid. The produced gas is reported for standard conditions (20°C, 1 atm) to account for the volume change with pressure. However, at operational top-side conditions between 3 and 10 bar, the measured GWR will be incomplete since not all the mass of gas will be released from the fluid. To assess this uncertainty in available data for geothermal doublets, the GWR based on production data (nlog.nl) is compared to available GWR measurements of bottom hole samples.

Table 2: Summary of gas data* from water and gas analyses (PVT) reports published on nlog.nl.

Well	Sampling point/Measurement method	Sample type	Sampling/opening pressure (bar)	GWR (-)	Bubble point (bar)	CO_2 (mol%)	CH_4 (mol%)	N_2 (mol%
LIR-GT-01	Bottomhole (BHS)	Pressurized liquid	-	0.8795	53.1	20.337	70.843	3.275
LIR-GT-01	Bottomhole (BHS)	Pressurized liquid	-	0.7197	44.2	13.227	78.822	3.571
LIR-GT-01	Surface - wellhead	Pressurized liquid	8	0.2471	10.1	56.717	39.344	0.415
LIR-GT-02	wellhead	Pressurized liquid	20.3	0.7494	41	22.299	66.915	4.207
MLD-GT01S1	Bottomhole (BHS)	Pressurized liquid	-	0.7751	48.3	15.506	80.54	1.989
MLD-GT01S1	not reported	Pressurized liquid	4.3 P opening	0.2156	6.6	28.024	58.462	10.13
BRI-GT-01	Bottomhole (BHS)	Pressurized liquid	205.5	1.0677	48.3	3.213	89.682	4.268
BRI-GT-01	Bottomhole (BHS)	Pressurized liquid	205.5	1.0821	48.6	3.412	90.538	3.412
BRI-GT-01	Surface - before the choke	Pressurized gas	3	-	-	2.1	92.926	2.155
BRI-GT-02	Surface - wellhead	Pressurized liquid	18	-	-	3.971	90.148	1.248
LSL-GT-01	Bottomhole (BHS)	Pressurized liquid	-	0.9894	77.2	3.871	92.858	1.933
LSL-GT-01	Unclear (probably surface)	unclear	7	-	-	2.913	86.54	8.567
PLD-GT-01	Surface - before the choke	Pressurized liquid	21.91 P opening	0.862	69	15.073	81.428	1.545
PLD-GT-01	Surface - before the choke	Pressurized liquid	25.68 P opening	0.936	76.5	11.046	81.264	5.173
PLD-GT-01	BHS	Pressurized liquid	-	0.576	29.6	6.449	88.786	2.427
PNA-01/02	Separator Gas Line	Pressurized gas	10	-	-	2.473	90.216	1.46
HAG-GT-01	Surface - Drill Pipe Manifold	Pressurized gas	6.9	-	-	1.697	93.074	2.424
HAG-GT-01	Surface - Drill Pipe Manifold	Pressurized liquid	6.96	-	91	3.371	77.86	1.521
HAG-GT-01	Surface - Drill Pipe Manifold	Pressurized liquid	7	-	75.8	5.292	88.521	2.037
HAG-GT-02	Surface - Separator Water Leg	Pressurized liquid	36	0.56	-			
HAG-GT-02	Surface - Separator Water Leg	Pressurized liquid	36	0.49	-			
HAG-GT-02	Surface - Separator Gas Line	Pressurized gas	36	-	-	6.518	89.579	1.324
HAG-GT-02	Surface - Separator Gas Line	Pressurized gas	36	-	-	6.508	89.542	1.334
HAG-GT-02	Calculated Separator GWR	Calculated		1.08				
HAG-GT-02	Calculated Stock tank GWR	Calculated		1.62				

HON-GT-01	Surface - Bypass	Pressurized gas		0.812	-	8.6	85.85	1.58
HON-GT-01	Surface - Bypass	Pressurized gas		0.896	-	8.92	85.64	1.71
HON-GT-01	Calculated GWR	Calculated		0.93	-	20.4	74.9	1.4
HON-GT-01	Calculated GWR	Calculated		1.01	-	19.1	76	1.5

*Samples with high air contamination as well as samples flashed at different pressures were excluded.
*Data for other hydrocarbons are excluded and hence the sum of the gasses does not add up to 100 mol%.

Table 3: Summary of fluid composition data and reservoir conditions taken from nlog.nl.

Well	Temperature (°C)	Pressure (bar)	Lab pH (-)	Cl^- (mg/)	Na^+ (mg/)	Ca^{2+} (mg/)	Mg^{2+} (mg/)	K^+ (mg/)	Sr^{2+} (mg/)	SO_4^{2-} (mg/)	Fe^{2+} (mg/)	Ba^{2+} (mg/)
LIR-GT-01	88	242	6.2-6.3	84000	32300	5180	786	230	307	198	111	6.2
MLD-GT01-S1	94	280	6.26	68000	40000	6200	680	340	350	270	84	6.1
BRI-GT-01	80	206	6	78000	43000	5900	900	630	356	330	76	4.2
LSL-GT-01	61	160	5.97	60000	34000	4200	770	280	300	150	33	27
HAG-GT-02	76	206	6.3	76000	39000	5460	900	2700	398	128	22	9.4
HON-GT-01	84	274	6.2-5.96	75710	38800	6190	983	458	373	200	72.1	8.24
PLD-GT-01	86	250	5.9	80600	50000	7200	1100	75	-	480	230	6.3
PNA-GT-05	76.5	200	6	87162	47540	5811	989	326	452	128	49	4

The production GWR is generally around a value of 1 (Table 4). Certain operators do not report a measured value but a derived value based on a fixed GWR as the value is constant with no variation. For example for LSL-GT-01, the GWR is fixed at 0.95 at pressures below 5 bar and at 1.00 for production pressures exceeding 5 bar. For MLD-GT-01 the GWR is first fixed at 1.00 for production at 5 bar, but after April 2020 the reported gas production appears to be measured and yields numbers around 1.1 at a 4 bar production pressure. For HAG-GT-01, the reported GWR is exactly 0.95 indicating it is not measured as well.

The calculated GWR based on flow data is valid for a certain range in system pressure (between 3 and 10 bar) at which not all gas is released from the fluid. Hence, this GWR is expected to be lower than a bottom hole samples GWR which is flashed at atmospheric pressures. However, the production GWR is in all cases (except HAG-GT-02) higher than the more accurate BHS GWR. This could indicate that the production GWR is quite inaccurate, although the BHS also have their uncertainties. The inaccuracy of the GWR based on the production data is illustrated by variation in reported GWR with operational separator pressure for the PNA and PLD sites. Although there is scatter, an increase of the calculated GWR with lower pressures is observed (Figure 5.1). The data for the PLD site indicates an increase in GWR of 0.1 for a 4 bar pressure decrease which is not large, but the data for the PNA site indicate that the GWR increases more than linearly towards atmospheric pressure.

Sampling at operational conditions will not only yield an incomplete GWR but will also result in deviations in the gas composition. Gasses can be sampled directly from the geothermal plant where free gas exists such as in the separator tank. Gas can also be sampled from a pressurised liquid sample which is outgassed in the lab. For both types of samples, the composition is affected differently, although both deviations are results of the solubility differences between CH_4 and CO_2. The solubility of CH_4 is lower than the solubility of CO_2 and hence the less soluble methane will preferentially outgas upon pressure decrease. Since pressurized liquid samples taken at the surface already have some gas escaped in the production well, they miss the escaped gas containing the highest CH_4 fraction. Therefore, pressurized liquid surface samples have an increased carbon dioxide fraction compared to bottom hole samples. This can be observed in the data, for example for LIR-GT-01 the CO_2 fraction is 13 and 20 mol % for bottom hole and up to 56.7 mol % for the surface sample. This illustrates how the CO_2 content in surface fluid samples represent a severe overestimation of the actual fraction in the reservoir fluid.

Table 4: Comparison of gas water ratios (GWR) determined by different methods.

Well	Sampling point/type	GWR (-)	GWR from measured production data	GWR from fixed value production data
LIR-GT-01	BHS	0.7197 - 0.8795	1.065	
MLD-GT01S1	BHS	0.7751	1.12	
BRI-GT-01	BHS	1.0677 - 1.0821		0.95
LSL-GT-01	BHS	0.9894		1.00
PLD-GT-01 PLD-GT-01	Surface BHS	0.936 0.576	1.06	
HAG-GT-02	Corrected GWR	1.62		0.95
HON-GT-01	Corrected GWR	0.93 - 1.01	0.985	

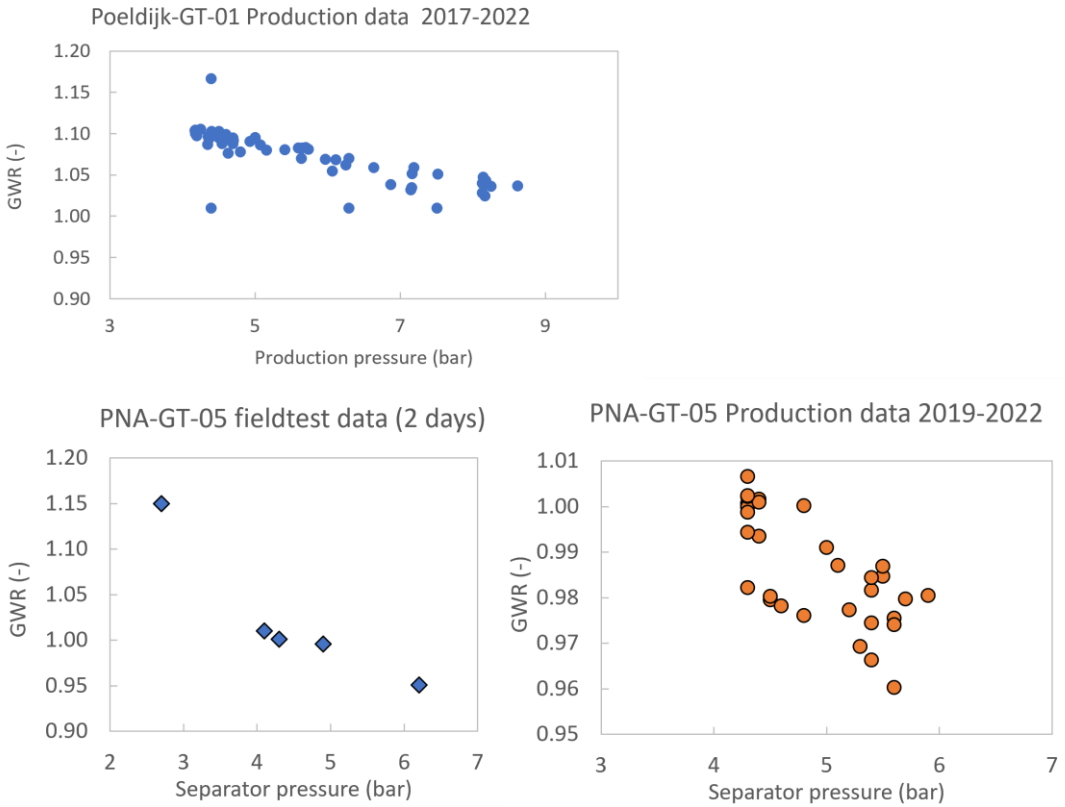

Figure 5.1: GWR based on the production for a range in top-side pressures.

Compared to the surface fluid samples, the deviation in measured gas composition is affected differently for gas sampled directly in the separator tank or the separator gas line. The gas released in the production well will end up in the separator tank, hence there is no free gas missing. However, a part of the gas will remain dissolved in the liquid and hence a gas sample from the separator tank will still be incomplete. Considering the higher solubility of CO_2 yielding relatively more CO_2 remaining dissolved, pressurized gas surface samples will have a lower CO_2 fraction compared to a bottom hole sample (and the pressurized liquid sample). This is illustrated for BRI-GT-01, which has 2.1 mol% CO_2 in the gas sample and 3.2 and 3.4 mol% in bottom hole samples. HAG-GT-01 also shows a lower CO_2 (1.7 mol%) in the gas samples compared to the surface pressurised liquid samples (CO_2 fraction of 3.4 and 5.3 mol%). For HON-GT-01 the GWR was measured in a bypass under operational conditions and later the amount of 'missing CO_2' was calculated. The 8.6 and 8.92 mol% CO_2 measured in surface samples was corrected to higher values of 20.4 and 19.1 mol% for reservoir conditions.

For the Pijnacker site a field test was done under varying operational pressure (Wasch et al., 2022). The test clearly illustrates the lower CO_2 fraction in the free gas in the separator tank with higher tank pressures (Figure 5.2). This effect of a low CO_2 content in the separated gas is enhanced for higher pressures in the separator tank, since higher pressures deviate more from the total outgassing at atmospheric conditions. Hence the lowest (separator) pressure gas composition is closest to the real value.

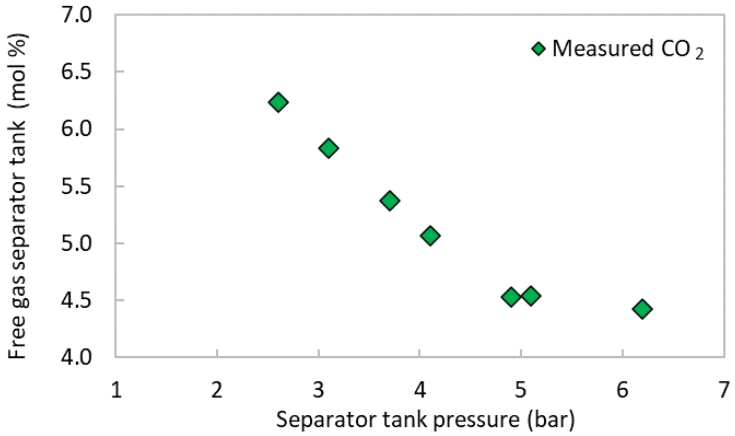

Figure 5.2: Change in the CO_2 fraction in the separated gas with varying pressures in the separator tank.

5.2 UNCERTAINTY IN FLUID COMPOSITION DATA

The fluid composition data for the selected sites (Table 3) are taken from water and gas analyses (PVT) reports published on NLOG.nl and collected in the Fluid Atlas. Analyses of the water composition of samples is not as complicated as gas content analyses. Changes in water composition due to cooling and depressurization resulting in mineral precipitation can be prevented by acidification of the sample. Hence the variation in measured water composition can be considered to reflect regional variations in fluid composition within the geological layers. The major elements show a variation of around 30% (Table 3). There are some outliers in the minor elements such as potassium and barium.

5.3 UNCERTAINTY IN FLUID PH DATA

A pH measurement is usually performed in the lab at a temperature of 20 to 25 °C and atmospheric pressure. This means that most CO_2 has been released from the solution and the pH will have changed accordingly. Following the reaction discussed before, the pH will increase with increasing CO_2 release (Formula 1). This means that all lab pH values are higher than the reservoir pH for the gas containing geothermal fluids. In addition, the equilibrium constant of water changes with temperature, yielding a higher neutral value for pH with the lower temperature in the lab. In the PERFORM project field test, the pH was measured in-situ with a bypass monitoring system as well as in the lab. The real time monitored pH was as low as 5.6 (depending on the amount of outgassing) while all lab pH measurements were around 6.0 (Wasch et al., 2022). This difference may appear small but will have a considerable influence on simulations of calcite scaling due to the pH sensitivity of this reaction. It is therefore important to include a correction of the lab pH value in the modelling workflow.

6 INCLUDING UNCERTAINTIES AND VARIATION IN GAS DATA AND PH IN SCALING PREDICTIONS

The determined uncertainties in gas composition and pH must be taken into account in numerical modelling. The WP4 results already showed that variation in fluid composition may significantly affect the accuracy of model simulations (Poort et al., 2022). For the case of calcite scaling the most influential parameters are the pH, the CO_2 content (partial pressure and volume) and the calcium concentration.

Firstly, the model-set-up and the assumptions on calcite equilibrium will be addressed. Secondly, base case model results for different sites will be discussed. Thirdly, a new method to deal with uncertainties is proposed.

6.1 MODEL DEVELOPMENT

6.1.1 Model set-up.

Modelling of scaling potential is performed with PHREEQC. Several steps are required to compute the scaling potential. The first steps are:

1. The measured solution composition is equilibrated with CO_2, CH_4 and N_2 at laboratory conditions. This is done because data of dissolved methane is usually not provided and since dissolved carbon data has significant uncertainties.
2. The measured volume of free gas is added to the solution at reservoir conditions (using a 'fixed pressure GAS PHASE' in PHREEQC), causing all the gasses to dissolve in the fluid. (This fluid is also equilibrated with quartz at reservoir conditions, since data for dissolved silica concentrations is often not available).
3. Check for the expected calcite equilibrium at reservoir conditions.

As discussed in the previous chapter the pH is affected due to degassing and cooling and the value obtained in the lab does not represent the pH of the original reservoir fluid. Step 2 and 3 of the model set-up account for this by re-introducing the gas, which results into a lowering of the pH. However, uncertainties in all measurements contribute to a deviation of the saturation state of calcite from equilibrium (step 3). With certain geothermal sites showing calcite supersaturation and certain sites showing calcite undersaturation. This has to be corrected for in order to produce coherent and accurate scaling predictions.

6.1.2 The assumption of calcite equilibrium (or saturation) in the reservoir.

PHREEQC simulations were run to find a more accurate pH to use as model input than the lab pH, to avoid under or supersaturation of calcite at reservoir conditions. The PHREEQC model contained and initial solution composition and an initial gas phase which were combined at reservoir conditions. The input pH of the initial solution was iteratively changed until the modelled saturation index of calcite at reservoir conditions became 0.

The assumption of equilibrium of the fluid and more importantly of the pH and the CO_2 partial pressure with calcite in the reservoir is crucial for the model set-up as well as for the subsequent development of the risk map. Equilibrium with calcite in a deep reservoir is generally considered realistic since carbonates react relatively fast. The presence of carbonates in the reservoir further supports the assumption of equilibrium, as shown for some of the sites included in this study. The mineralogical composition of cuttings was determined and indicated that calcite is a commonly occurring mineral in the reservoir (Wasch et al., 2020).

Table 5 lists the original lab pH and the iteratively changed initial solution pH to achieve calcite equilibrium in the reservoir. The simulated final pH at reservoir conditions represents the pH of the reservoir fluid before degassing. Note that the corrected pH depends on the CO_2 partial pressure and the volume of gas. For example, a higher CO_2 partial pressure requires a higher pH to compute calcite equilibrium in the reservoir. Hence any uncertainties in these values are transferred to the corrected pH. These uncertainties will be addressed in chapter 6.3.

Table 5: Overview of measured, corrected and simulated pH values.

	LIR	MLD	BRI	LSL	HAG	HON	PLD	PNA
Lab pH (-) at 20-25 °C and 1 atm.	6.2-6.3	6.26	6	5.97	6.3	6.2-5.96	5.9	6
Model input: Initial solution pH (-) Corrected to achieve SI Calcite = 0 at reservoir P/T	5.764	5.77	6.2	6.37	6.27	5.8	5.87	6.015
Model output: pH (-) at reservoir P/T	5.198	5.263	5.587	5.797	5.535	5.191	5.255	5.452

6.2 SITE SPECIFIC MODEL RESULTS FOR CALCITE SCALING POTENTIAL

The outgassing process with pressure decrease and the related scaling potentials have been modelled for the different sites (Figure 2.2,). The site specific data (Table 1, Table 2 and Table 3) is used to make the base case models, the uncertainties will be included in the following section. The different options for the GWR (used as input for the gas volume) discussed in section 5.1 are taken into account as a first indication of the effect of uncertainties.

The site-specific model results are presented in Figure 6.1. The results are split in two figures, for the sites with the GWR based on production data for the sites with available BHS GWR values or corrected GWR values. No gas is released upon the first pressure decrease in the production well (Figure 6.1a and b). For each site, the pressure for which gas starts to escape the fluid (the bubble point) is different. With pressures below the bubble point, more and more gas is released and the pH increases as result (Figure 6.1c and d) and the calcite scaling potential, expressed as the calcite saturation index, also increases (Figure 6.1e and f). For all models the calcite saturation index shows supersaturation at all pressures. Note that the full pressure range is not shown for the saturation index (Figure 6.1e and f), but that the SI reduces to 0 at the reservoir pressure. How the predicted calcite supersaturation with pressure release relates to a scaling risk will be discussed in chapter 7.

The corrected bottom hole GWR of HAG is quite high which yields the highest amount of outgassing and the highest predicted scaling potential (Figure 6.1a and e). A higher amount of outgassing and a high pH do not necessarily result in the highest calcite supersaturation. For example, LSL has a relatively high pH but low Calcite SI since this site has the lowest reservoir temperature of only 61 °C. The effect of different GWR's is most pronounced for the HAG site, with the production data GWR yielding a calcite SI of 0.8 and the BHS GWR input yielding a SI of 1.0 at 1 bar (Figure 6.1e compared to f). For MLD, the higher production GWR yields a 0.1 higher calcite SI and for De Lier only a 0.07 higher calcite SI (results not shown). For the Pijnacker site, a second GWR of 0.7 was determined by matching the gas volume with the measured pH and CO_2 concentration reported for a field test (Wasch et al., 2022). The differences in resulting pH and calcite SI are quite small (Figure 6.1d and f).

For certain sites we have good data on fluid and gas compositions while for other sites this data can be incomplete or of poor quality. In the following section, the effect of these uncertainties will be investigated for all sites.

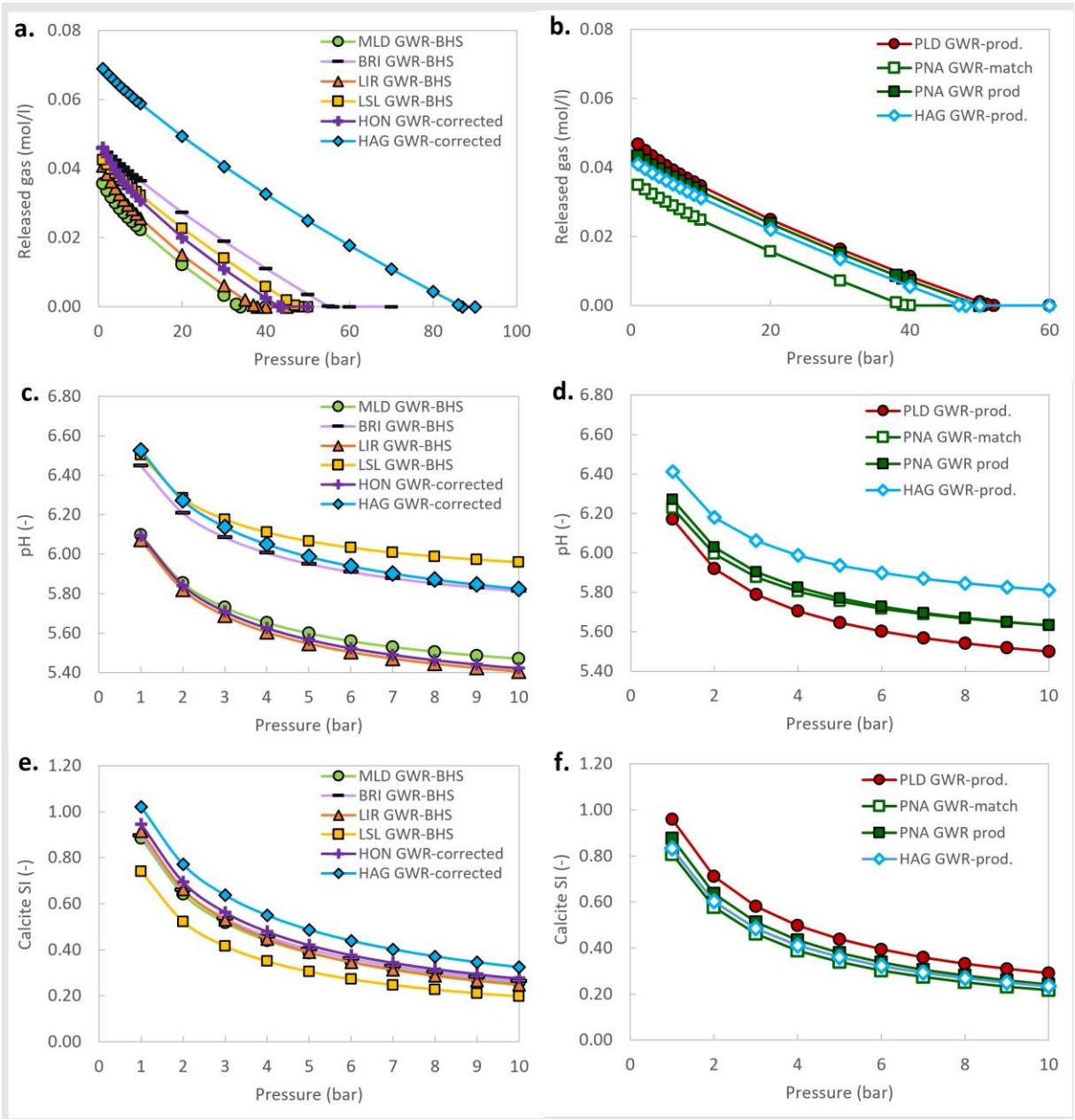

Figure 6.1: Site specific model results showing a/b) the amount of released gas with pressure decrease, c/d) the simulated pH and e/f the resulting calcite scaling index.

6.3 PROPOSED NEW METHOD FOR UNCERTAINTY REDUCTION

The uncertainty quantification tool was used to include the defined uncertainties and variations in fluid pH and CO_2 content. The tool randomly varies a defined nominal pH value and CO_2 partial pressure and runs the geochemical model for each input set to calculate the saturation index of calcite. By performing a large number of such calculations with randomly sampled input parameters, the impact of uncertainties on scaling risks can be determined. A range in pH and CO_2 partial pressures was defined that encompasses the variation in measurements (Table 2 and Table 3).

As a first step, the model was run at reservoir conditions to find the range in pH and CO_2 partial pressures that meet the constrain of calcite equilibrium in the reservoir. As expected there is a relationship of higher pH and a higher CO_2 partial pressure (corresponding to a lower value of the log value of the partial pressure) resulting in a higher calcite SI (Figure 6.2a and b). Yet almost the entire range of pH and CO_2 partial pressure can yield calcite equilibrium in the reservoir. However, when output data is filtered on calcite equilibrium (SI between -0.01 and 0.01) as shown by the black rectangles in Figure 6.2a and b, the input values are reduced from the full spread (Figure 6.2c) to a single line (Figure 6.2d). This line represents all the input combinations that yield a calcite SI of ~0 and originates from the principle that with a fixed calcite saturation index, a higher pH requires a lower CO_2 partial pressure – and vice versa – to retain equilibrium.

The second modelling step computes the calcite scaling tendency at a reduced top-side pressure of 2 bar. Using the entire range of input values (Figure 6.2c) yields a very large range in saturation index (Figure 6.2e), from undersaturated (-0.8) to supersaturated (2.0). With such a large range no meaningful risk assessment can be done. Selecting only input combination that fall on this 'SI=0 line' greatly improves the predictions of scaling risks. With these sets of input parameters (Figure 6.2d), a much smaller range of scaling tendencies is predicted, between SI 0.67 and SI 0.71 (Figure 6.2f). Since all the input combinations that do not comply with the condition of calcite saturation in the reservoir are excluded, this smaller range in calcite risk is more realistic.

The function between pH and CO_2 partial pressure can be used to select the realistic input parameters from the randomly generated combinations of pH and CO_2 partial pressure input values. With all the combinations of pH and CO_2 partial pressure ı input parameters that fall on this function (Figure 6.2d), roughly the same scaling index is modelled. This means that it is not required to precisely know these often poorly constrained parameters in order to achieve a precise prediction of the scaling tendency. This is a powerful method to evade uncertainties in fluid and gas compositions. With only the more easily determined solution composition and together with the reservoir conditions, the carbonate scaling risk can now be accurately determined.

To implement this method, a new functionality was added to the uncertainty tool to generate sets of input parameters from the defined function. By using the defined function and the randomly generated values of CO_2 partial pressure, the appropriate pH values will be calculated. These new pH values will still contain a random variation to them; however, the input pH and CO_2 partial pressure values will now satisfy the 'SI=0' condition. The tool can still be used to add random variations in fluid chemistry.

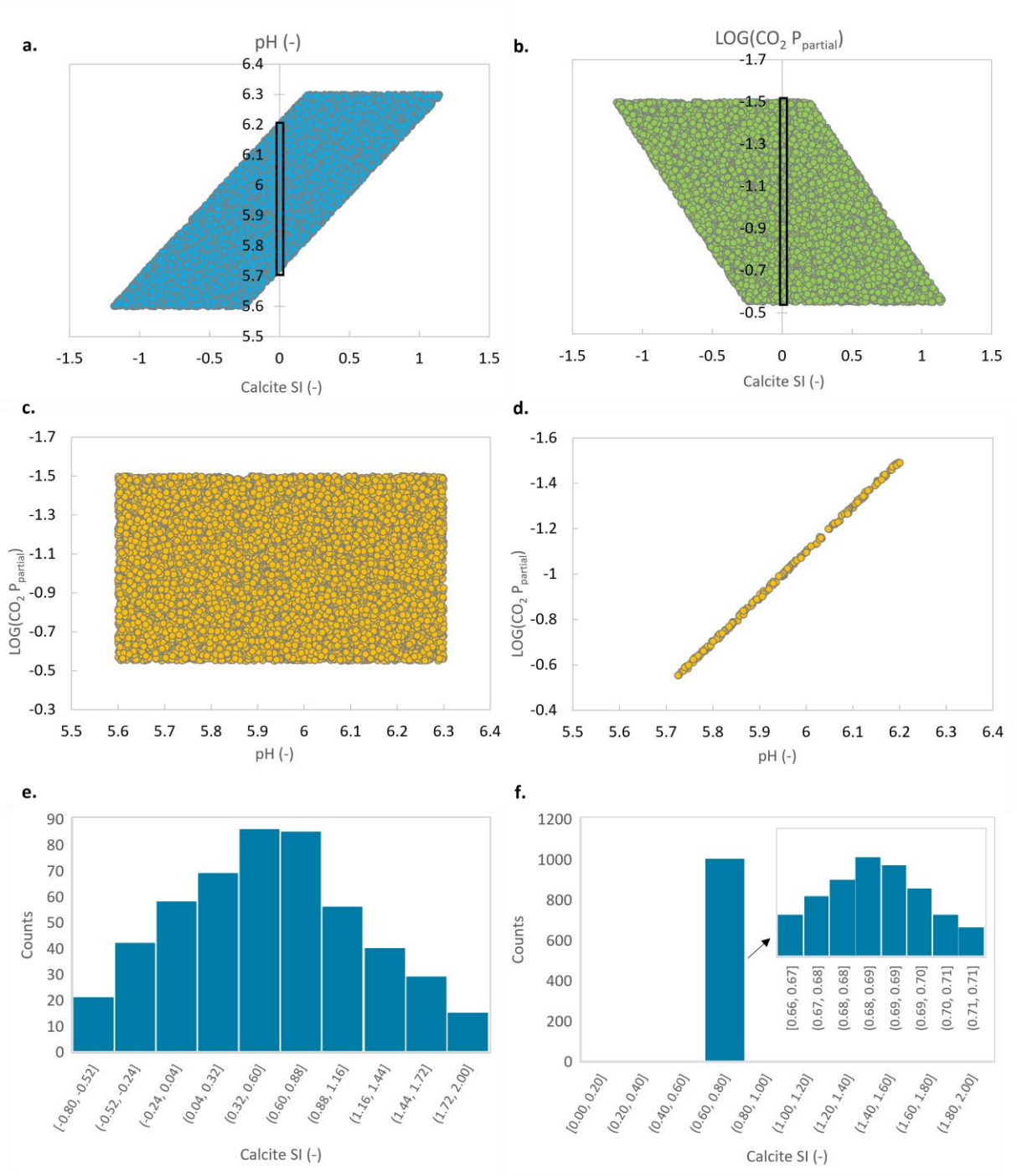

Figure 6.2: Example of the uncertainty reduction workflow for the Honselersdijk case.

6.4 TESTING THE UNCERTAINTY REDUCTION WORKFLOW ON THE SITE-SPECIFIC MODELS

The uncertainty reduction workflow is tested on the site-specific models. Instead of their site-specific pH and CO_2 partial pressure, these input values were randomly varied within the total range in measured pH and CO_2 partial pressures (Table 2 and Table 3). Each site-specific model was run for 10000 sets of input parameters. The function between pH and CO_2 partial pressure is determined for which the calcite SI is between -0.01 and 0.01. This is done by filtering the output on calcite equilibrium after which about 100 to 200 input combinations are left. A linear trendline is used to define the function (Figure 6.3 and Table 6). As expected each site has a specific function between pH and CO_2 partial pressure valid for their reservoir pressure and temperature conditions and the fluid composition.

The effect of temperature is evident, with the lowest temperature of Lansingerland (61 °C) and the highest temperature of Maasland (94 °C) representing the maximum and minimum functions (Figure 6.3). This indicates that the temperature poses a strong control on the determined functions. The functions between pH and CO_2 partial pressure are not exactly ordered by temperature, which shows the second order effect of fluid composition.

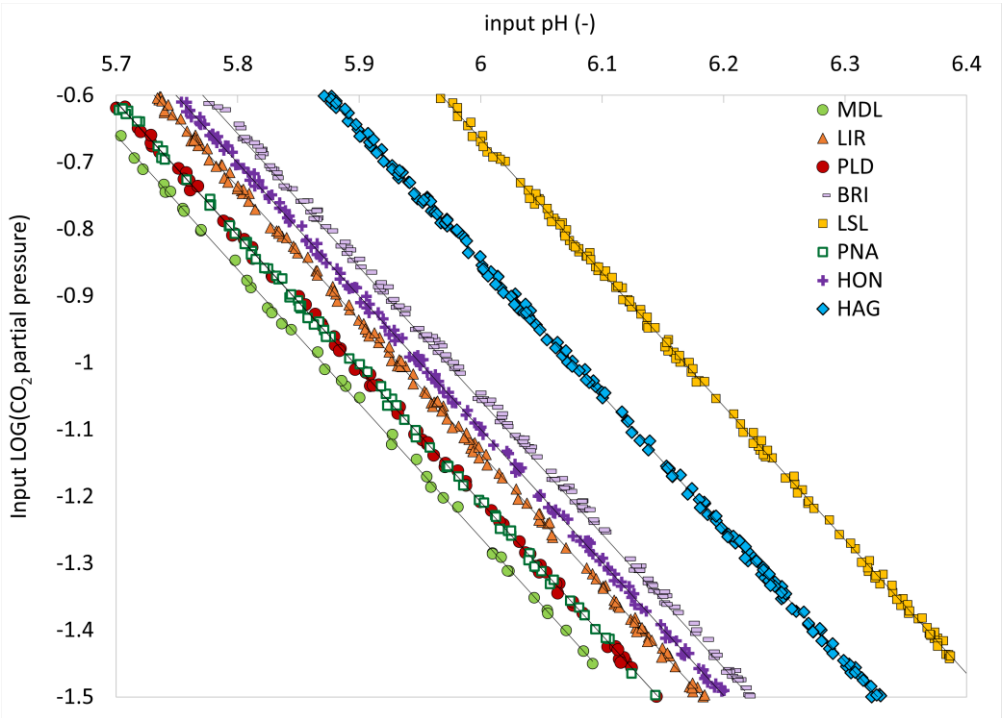

Figure 6.3: Linear functions between pH and CO_2 partial pressure defined for each site.

The updated uncertainty quantification tool is used to calculate the saturation index by sampling input parameters only from the linear function. 2000 random samples were run to assess the remaining uncertainty on scaling predictions. The scaling potential is defined for 2 (top side separator tank) pressures of 2 bar and 4 bar instead of the full pressure range from reservoir to atmospheric. Each determined scaling potential is an average of 2000 runs and shows a very small variation of less than 3 % (Table 6). This illustrates how by using these functions, one precise value for the scaling risk can be determined.

To assess the accuracy of the uncertainty reduction workflow, the calcite SI results are compared for the site-specific pH and CO_2 partial pressure and the pH and for CO_2 partial pressure functions. There are only small deviations of less than 2% when comparing the SI based on the function describing the entire pH-CO_2 range and the SI from the site specific models (Table 6 compared to Figure 6.1e and f). This shows that the functions can be reliably used to predict scaling risks without site specific data on pH and CO_2 partial pressure.

As seen in the site-specific model results, the calcite supersaturation defined using the pH-CO_2 function increases with lower pressures from 4 to 2 bar (Table 6), following to the larger amount of gas release at lower pressures. There is a rough relation of lower reservoir temperatures yielding lower supersaturations, with LSL (61 °C) having the lowest calcite SI. The high (unconfirmed) GWR of the 'Den Haag corrected' yields a high calcite SI, while using the production data GWR yields the second lowest calcite SI which agrees with its relatively low temperature (76 °C). Hence there is a strong control of temperature on the predicted scaling tendency. On top of the temperature control, there are influences of the fluid composition.

Table 6: The linear functions for each site with the resulting scaling SI and variations.

Site	Data source GWR	Fitted trendline (y= LOG(CO_2 $P_{partial}$), x =pH)	Calcite SI @ 2bar	Calcite SI @ 4bar
Maasland (MDL)	BHS	y = -2.0063x + 10.776	0.64 ± 3%	0.44 ± 0.5%
De Lier (LIR)	BHS	y = -1.9931x + 10.823	0.65 ± 3%	0.45 ± 0.5%
Brielle (BRI)	BHS	y = -1.9967x + 10.923	0.66 ± 2%	0.46 ± 1%
Lansingerland (LSL)	BHS	y = -1.9993x + 11.331	0.53 ± 2%	0.35 ± 2%
Honselersdijk (HON)	corrected	y = -1.9909x + 10.846	0.69 ± 2%	0.48 ± 1%
Poeldijk (PLD)	Surface sample	y = -1.9959x + 10.767	0.71 ± 2%	0.49 ± 0.5%
Pijnacker (PNA)	production	y = -1.9952x + 10.820	0.65 ± 2%	0.44 ± 1%
*Pijnacker (PNA)	matched	y = -1.9923x + 10.745	0.58 ± 3%	0.39 ± 2%
Den Haag (HAG)	corrected	y = -1.9905x + 11.093	0.78 ± 1%	0.55 ± 1%
*Den Haag (HAG)	production	y = -1.9955x + 10.974	0.61 ± 2%	0.41 ± 1%

To better assess how the functions are affected by fluid composition, two models were made with different compositions representing the range of Delft fluid compositions (Table 3). To exclude the effect of temperature, both models have the same reservoir conditions (274 bar, 85 °C). It was decided not to use the uncertainty quantification tool to generate a full range in fluid composition since fluid compositions are not random and uncorrelated. The fluid compositions in Table 3 show that in general high potassium chloride brines also have high calcium, magnesium, strontium and sulphate concentrations.

To assess purely the effect of variation in fluid composition, two fluid compositions are defined for relatively high and low salinity brines (Table 7). These represent the maximum and minimum values measured for the Delft (Table 3). For a pressure decrease from reservoir pressure of to 2 bar, the predicted calcite saturation index is 0.68 for the minimum salinity model and 0.70 for the maximum salinity model. This small difference indicates that the fluid composition is of less influence compared to the temperature.

Table 7: Compositions of the defined maximum and minimum salinity fluids.

	Cl^- (mg/)	Na^+ (mg/)	Ca^{2+} (mg/)	Mg^{2+} (mg/)	K^+ (mg/)	Sr^{2+} (mg/)	SO_4^{2-} (mg/)	Fe^{2+} (mg/)	Ba^{2+} (mg/)
Maximum salinity	88000	39000	7200	1100	500	450	500	230	10
Minimum salinity	60000	39000	4200	650	200	300	125	20	4

7 SCALING RISK MAPS

To provide improved recommendations for scaling prevention, risk maps are made. A risk map contains predictions of scaling beyond the site specific and can be an important step towards improved operational advice and enhanced geothermal energy production. The new model approach can include uncertainties and variations, while still retaining accuracy and precision in calcite scaling predictions.

The previous model exercises showed that the reservoir temperature has the strongest control on the scaling potential predicted for the reservoir fluid during production to the surface. It was concluded that the fluid composition has only a small control on the scaling potential (within the variation observed for the Delft sandstone). Hence the reservoir temperature is used as the main indication of the scaling risks. The ThermoGIS temperature map of the Delft and Alblasserdam members will be used as the base of the risk map.

7.1 DEFINING SCALING RISK

All model predictions indicate calcite supersaturation upon production of the reservoir fluids to the surface. Before a risk map can be made, a risk evaluation has to be assigned to these predicted supersaturations. There is a risk of scaling when the predicted supersaturation exceeds the supersaturation required to overcome the kinetic inhibition for nucleation and crystal growth, and calcite starts to precipitate. The saturation at which calcite starts to precipitate is called a critical saturation index or a critical saturation ratio (e.g. Ramstad et al., 2020 and Malik et al., 2007). Experiences of calcite precipitation in the field have to be linked to simulated scaling supersaturation to find this critical saturation index.

For the West-Netherlands basin, one case is known of severe calcite scaling. Carbonate scaling was observed in the Pijnacker geothermal plant when the pressure was reduced to 2 bar in an oil and gas separator tank (Wasch et al., 2022). The critical saturation index for the Pijnacker is thus the amount of supersaturation at 2 bar. With the site specific model a critical scaling index between 0.58 and 0.64 was determined for the Pijnacker site (PNA), depending on the GWR (Figure 6.1). Using the uncertainty reduction method with the pH-CO_2 function, the determined critical scaling index is almost the same (between 0.58 and 0.64, Table 6). The more the critical scaling index is exceeded, the higher the calcite scaling risk, since calcite kinetics and deposition are faster at higher temperatures.

At higher system pressures of 4 bar, no carbonate precipitation was observed at the Pijnacker site (Wasch et al., 2022), and the related supersaturation will relate to no scaling. Supersaturations between 0.39 and 0.44 (Table 6) and lower hence indicate a low scaling risk.

The calcite saturation index and hence the scaling risk is pressure dependant, since calcite precipitation is triggered by pressure decrease and outgassing. Therefore, risk maps should be made for certain operational conditions such as the lowest pressure in the geothermal plant.

7.2 SCALING RISK MAP WORKFLOW

A workflow is proposed to create risk maps:

1. One fluid composition is used with median values of the Delft Sandstone fluid compositions (Table 8).

Table 8: Fluid composition of the risk map model.

	Cl	Na	Ca	Mg	K	Sr	SO_4^{2-}	Fe	Ba
mg/l	76000	39000	5900	900	340	353	200	76	6.3

2. The model was run for different P/T conditions of the Delft and Alblasserdam reservoirs (Table 9). The temperature ranges were defined based on the ThermoGIS temperature map (Figure 2.2). The corresponding pressures were based on the temperatures following a geothermal gradient of 31 °C/km (Table 9).

Table 9: Temperature ranges and corresponding models for the risk map.

ThermoGIS T ranges		PHREEQC model P/T conditions			
Ranges	Min-Max T (°C)	Models	T (°C)	Depth (km)	P (bar)
Range 1	25 - 40	Model 1	40	1.29	129
Range 2	40 - 55	Model 2	55	1.77	177
Range 3	55 - 70	Model 3	70	2.26	226
Range 4	70 - 85	Model 4	85	2.74	274
Range 5	85 - 100	Model 5	100	3.23	323

3. For the P/T conditions of models 1 to 5, a linear function between the input pH and CO_2 partial pressure is determined. Each model is run 10000 times with randomly selected pH and CO_2 partial pressure input parameters. For each model, the results are filtered on the assumption of calcite equilibrium ($0.01 < SI > -0.01$) and with a trendline through the remaining values, the temperature specific function between pH and CO_2 partial pressure is obtained.

4. For each P/T model, a scaling model was made using the updated uncertainty quantification tool to sample input parameters from the pH and CO_2 partial pressure linear function. The models were run for 2 and 4 bar pressures (and no cooling) to assess the scaling risks for different top-side operational pressures.

5. The scaling risks for the different temperature ranges were assigned to the temperature map to visualize the predicted scaling risks on a regional scale. The scaling risks were defined by how much the saturation index of calcite deviates from the

critical scaling index of the Pijnacker site (PNA) of around 0.6. A scaling risk map will be valid for a specific outgassing pressure in the geothermal plant.

7.3 DEMONSTRATION OF CALCITE SCALING RISK MAPS FOR THE WEST-NETHERLANDS BASIN

Following the risk map workflow, the models for the different temperature/pressure conditions in the reservoir were run 10000 times to obtain an accurate function between pH and the CO_2 partial pressure (Table 10). By sampling 2000 random sets of input parameters from the functions with the full range of possible input parameters, an average value for scaling is determined with less than 4% variation. For depressurization at 2 bar, the simulated calcite saturation index shows a temperature dependence with values of 0.43 up to 0.76 for temperatures of 40 °C up to 100 °C. Although the simulated calcite saturation index is lower for 4 bar, the same range of SI change with is observed, with the 100 °C model showing a 0.3 higher SI than the 40 °C.

Table 10: The linear functions for 5 P/T conditions and the scaling SI at 2 and 4 bar.

Models	T (°C)	P (bar)	Fitted trendline (y= LOG(CO_2 $P_{partial}$), x =pH)	Calcite SI @ 2bar	Calcite SI @ 4bar
Model 1	40	129	y = -1.9952x + 11.302	0.43	0.27
Model 2	55	177	y = -1.9908x + 11.148	0.53	0.35
Model 3	70	226	y = -1.9903x + 11.0	0.62	0.42
Model 4	85	274	y = -1.9937x + 10.863	0.70	0.49
Model 5	100	323	y = -1.9918x + 10.686	0.76	0.54

The determined values for the calcite scaling index were visualised on a map (Figure 7.1 and Figure 7.2). The scaling risks were defined by how much the modelled calcite SI deviates from the critical scaling index of ~0.6 as determined for the Pijnacker site. Regions with a SI below the PNA critical SI have a low scaling risk and regions with an SI exceeding the critical SI have a high scaling risk. The colour scale indicates high to low scaling risks with purple/red representing a high scaling risk, orange a medium scaling risk and green/blue a low scaling risk (Figure 7.1 and Figure 7.2).

With a low top side pressure of 2 bar, the scaling risk is high for most of the West-Netherlands Basin (Figure 7.1). Only the low temperature North-Eastern part has a low scaling risk. With a higher top side pressure, only the most Western part of the West Netherlands Basin has a high scaling risk. This indicates that a pressure of 4 bar in the separator tank is high enough to prevent calcite scaling for most of the West Netherlands Basin and that only fluids from reservoirs with temperatures above 80 °C require a higher system pressure to prevent scaling.

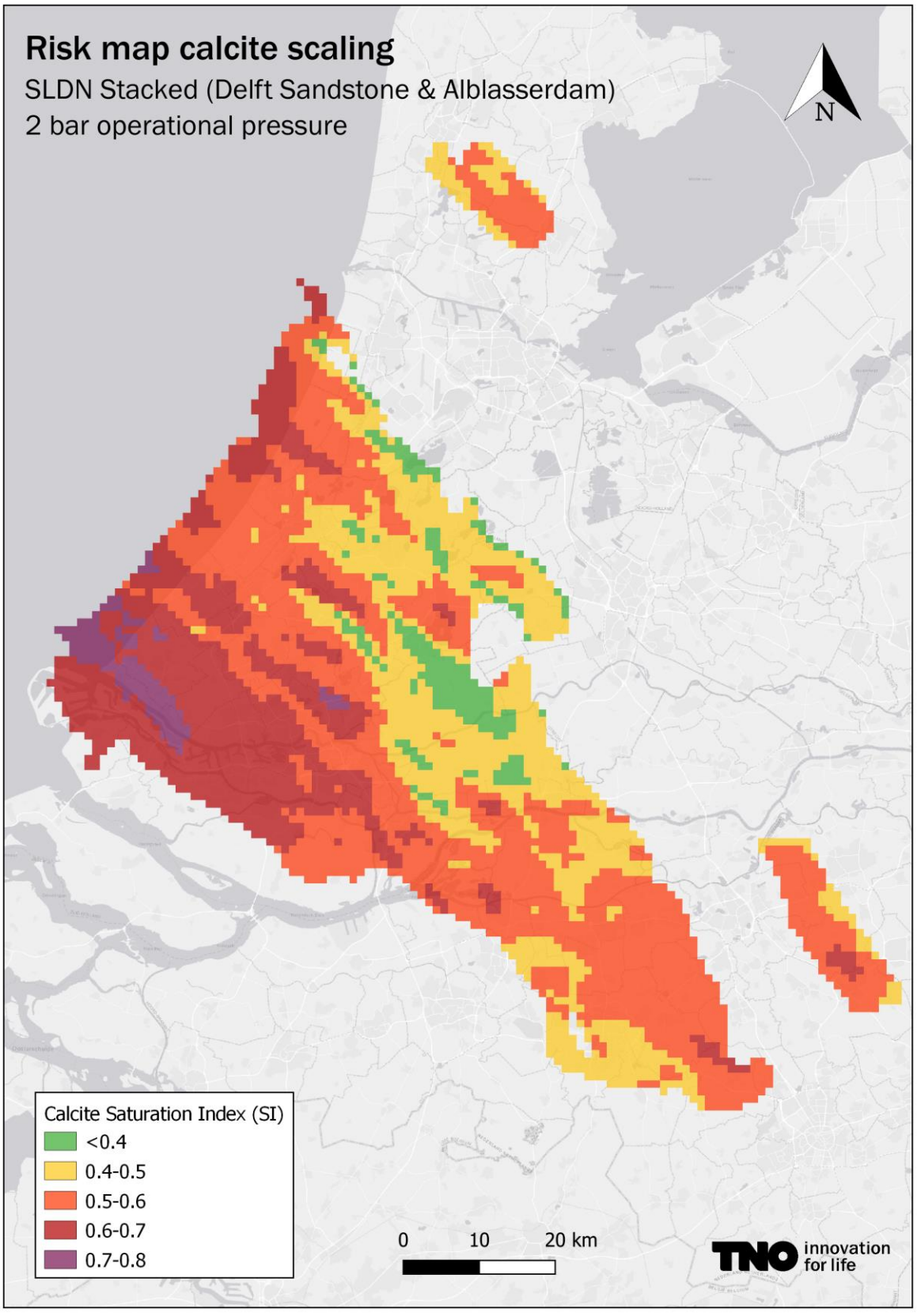

Figure 7.1: Calcite scaling risks at 2 bar.

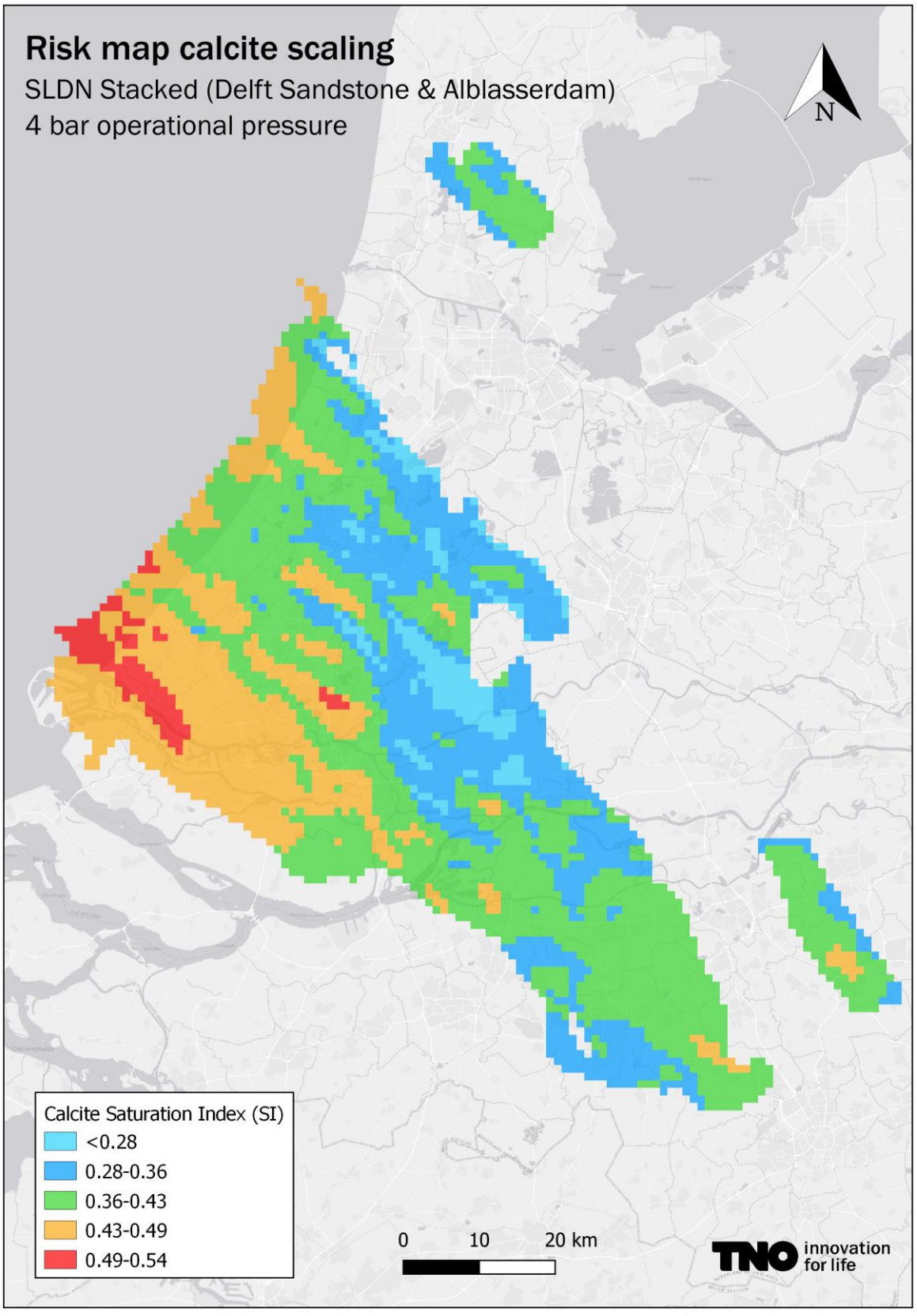

Figure 7.2: Calcite scaling risks at 4 bar.

8 DISCUSSION

The workflow for the risk map is very powerful for dealing with uncertainties and natural variations in pH and gas composition, reducing these uncertainties to almost zero within geological reservoirs of similar characteristics. Uncertainties and variations in fluid composition result in very small uncertainties in scaling predictions of only less than 2%. The uncertainty that is more challenging to assess is the uncertainty on the risk itself, or more specifically on the risk assigned to a certain scaling index. The current definition of high and low scaling risks relies heavily on the experience of one field case (Wasch et al., 2022). Based on this case, the defined calcite saturation index that represents a high scaling risk is 0.6. This is the critical saturation index at which calcite is sufficiently supersaturated to overcome any inhibitions in nucleation and kinetics and precipitates. One value for SI was selected, but the critical saturation state may have a temperature dependence since at high temperatures kinetics are faster and precipitation will be less inhibited. In addition, the composition may contain inhibiting ions at larger or smaller concentration.

Ramstad et al., 2020 provided an overview of critical saturation index (defined as saturation ratio by the authors) for actual experiences with $CaCO_3$ scale formation in oil and gas fields in the North Sea and Norwegian Sea. The observations of scale formation and non-scaling conditions were correlated to thermodynamic calculations and it was concluded that high-pressure, high-temperature fields have higher scaling risks. Similar to pressure decrease at the surface during geothermal production, oil and gas fields may experience high pressure drawdown from the reservoir into the well which increases the risk of $CaCO_3$ scaling. The critical SI defined for these oil and gas fields is between 0.11 and 0.68 for temperatures between 77 °C and 110 °C (Table 11). Since these temperatures are comparable to the Delft reservoir, this data supports the determined critical SI of ~0.6 for the Pijnacker site. There is no clear correlation with temperature based on the data in Table 6, so this data cannot be used to determine an exact temperature correlation for the critical saturation index. It however indicates that the values deduced for the PNA site is likely not valid under all geothermal conditions.

From experiences with calcite scaling related to gas production in mature oil fields, Malik et al., 2007 defined a critical saturation ratio of 2-3 (which corresponds to a critical SI 0.3-0.5) for temperatures below 100 °C and a critical saturation ratio of 1.2 (which corresponds to a critical SI of <0.1) for higher temperatures. For much lower temperatures, data from hot springs can be used, for which a critical saturation index of calcite was determined between 0.7 to 0.9 for temperatures between 15 and 45 °C (Sasaki et al., 2009). This high critical saturation index for low temperatures is supported by Ramstad et al., 2020, who defined a critical SI between 0.7 and 0.9 for fluids of 60 °C, based on data of seawater heating.

Table 11: Selection of data from Table 1 of Ramstad et al., 2020 and references therein, the saturation ratio is recalculated to SI for easy comparison following SI=LOG(SR).

Field	T (°C) scaling location	Minimum $SI_{critical}$	Maximum $SI_{critical}$
Brage	77	0.26	0.33
Oseberg Sør	82	0.41	
Stjerne	85	0.26	
Hitchcock	91	0.40	
Oseberg C	93.8	0.38	0.59
Zelda	99	0.39	0.62
Oseberg Sør	99	0.11	0.42
Farida	104	0.40	0.68
Visund	105	0.16	0.31
Yme	110	0.13	0.20

Although the change in critical saturation index (also reported as critical saturation ratio SR) with temperature as reported in literature is not always precise, a general trend can be defined of:

- > 100 °C: high reservoir temperature critical SI of 0.1 to 0.3 (critical SR 1-2)
- 60 - 100 °C: medium reservoir temperature critical SI of 0.3 to 0.7 (critical SR 2-5)
- 15 – 60 °C: low reservoir temperature critical SI 0.7 to 0.9 (critical SR 5-8)

All of the selected sites in the West Netherlands Basin fall in the medium reservoir temperature range with a critical saturation index of 0.3 to 0.7. This indicates that using the critical SI from PNA should not result in large uncertainties regarding the higher and lower temperatures of the other sites. In general, the higher temperature sites would have a lower critical saturation index and hence the computed scaling index would exceed the critical SI more, which yields a higher risk. Another note on the temperature effect is that any cooling in the well before outgassing (which could be a couple of degrees), will reduce the scaling risk slightly.

Risk can be defined as the probability times the impact of a certain event, calcite scaling in our case. When considering risk, we have considered the probability of scaling to occur when considering uncertainties. The impact of scaling depends on the amount of scaling and whether large volumes of scaling occur that decrease flow or heat transfer in the geothermal plant. At Pijnacker the impact of scaling was severe when a top side pressure of 2 bar was applied, for which a critical saturation index of around 0.6 is determined. A critical saturation index is a critical value for scaling to occur, but the higher the saturation index the more the severe the scaling can be since deposition is faster. Ness at al., (2021) found mild scaling at for a saturation index below 0.11 and severe scaling with a saturation index between 0.4 and 0.85, similar to the PNA site. Karabelos, 2002 found that at supersaturations below a critical

saturation index of 0.85, the deposition rate is small and above this value there is sharp rise in deposition rate. However, it has to be considered that with the large volumes of water production in geothermal plants, a slow deposition rate may still add up to large volumes of scale deposition in the course of time.

Ramstad et al., 2020 also provided a method for risk assessment and operational advice. They made an operational risk diagram where the critical saturation index based on thermodynamic calculations were plotted against the downhole temperatures to indicate regions of high, medium and low risk. The operational risk diagram shows another example of the power of these calculations for scaling management. The diagram is a convenient way of assessing scaling risks but it requires a lot of data points of wells with (and without) scaling which we do not have for the West-Netherlands basin scaling case.

The presented risk maps are made for calcium carbonate while other carbonates have been found such as iron carbonate (Pijnacker, personal communication). The precipitation of precursor amorphous phases or other carbonates or the pure calcium carbonate polymorphs vaterite, aragonite, calcite may affect the risk map. Different carbonate minerals or polymorphs will have their own mineral specific critical saturation index at a specific temperature. For example, a critical saturation index between 0.25 and 1.14 was determined for magnesite at 100 °C (Giammar et al., 2005). A higher critical saturation index of 2.0 was determined for magnesite formation following experiments at 100 °C as well but at a higher CO_2 pressure of 100 bar (Wang, 2013). For much lower temperatures between 15 and 45 °C, Sasaki et al. (2009) mentioned values of 3.5 for dolomite, 0.5 for magnesite, 1.2 for siderite and 3.4 for dawsonite.

It is concluded that for each scale mineral a separate risk map must be created for a temperature and pressure specific critical saturation index. Hence the created scaling risk map in this study can only be used to assess risks of calcite scaling and not for other minerals.

9 CONCLUSIONS AND RECOMMENDATIONS

In this chapter, the main conclusion of the work performed within the work package will be given and suggestions for future work are provided.

9.1 FLUID SAMPLE COMPARISON USING PCA

The dimension reduction technique of principal component analysis (PCA) was applied to fluid compositions from the REFLECT fluid sample database. This type of analysis allows for comparison between sites not only on geographical location, but also on brine composition. A tool was developed on top of these methods that allows the user to define their own fluid composition and compare it to all other sites in the database in order to find similar wells and potentially anticipate on common (known) risks associated with these wells such that they could be mitigated/prevented for the well owner/operator in question. The tool is freely available for all partners in the REFLECT project[2].

In the future, to improve the actionability of the comparison analysis, it would be useful to compile a list of common or known brine-related operational issues per site or group of wells and include them in the fluid sample database, such that it is easier to find and anticipate on potential expected issues when comparing a user's well to the wells in the database.

9.2 SCALING RISK MAP

The main objective of the risk map is to provide an assessment of scaling risks where no data yet exists. This provides future operators with recommendations on how to best design and operate their geothermal systems for scaling mitigation. The Fluid Atlas provides an excellent opportunity to access regional fluid data and to use that data for regional scale risk assessment. The quality of the risk map is directly related to the quality of the data and the reliability of numerical models.

There are large uncertainties and variations in the measured fluid pH and the gas composition. However, these values are especially important to know accurately since the pH and the CO_2 partial pressure directly control the solubility of calcite. A new method is defined to reduce the uncertainties in fluid and gas data and subsequent scaling predictions. The method is based on the relation between pH and the CO_2 partial pressure for a fixed saturation index for calcite. To retain equilibrium of calcite (a saturation index of 0), a higher pH will require a lower CO_2 partial pressure and vice versa, which forms a linear relationship. Furthermore, with any set of pH and CO_2 partial pressure from this linear function, the same amount of calcite scaling will be simulated (< 4% error). This means that it is not required to precisely know

[2] Please contact jonah.poort@tno.nl for access and more information or questions.

these often poorly constrained parameters in order to achieve a precise prediction of scaling risks. This is a powerful method to evade uncertainties in fluid and gas compositions. With only the more easily determined solution composition and reservoir conditions, the carbonate scaling risk can now be accurately determined.

The site-specific model results show that the pH-CO_2 partial pressure function depends on the temperature and pressure conditions in the reservoir and to a lesser extent on the fluid composition. The function does not depend on volume within the range of observed GWRs (~20% variation). Since the temperature appears to have the largest control on the predicted scaling tendency, a risk map can be made based on the temperature map. Risk maps for calcite scaling have to made for a specific top side pressure since the scaling risk is related to outgassing due to pressure decrease.

The workflow for making the risk map is demonstrated for the geothermal doublets targeting the West Netherlands basin. With a low top side pressure of 2 bar, the scaling risk is high for most of the West Netherlands Basin. Only the low temperature North-Eastern part has a low scaling risk. With a higher top side pressure of 4 bar, only the most Western part of the West Netherlands Basin has a high scaling risk. The risk map indicates that a pressure of 4 bar in the separator tank is high enough to prevent calcite scaling for most of the West Netherlands Basin and that only the region with temperatures above 80 °C requires a higher system pressure.

10 REFERENCES

Balen van, R., Van Bergen, F., De Leeuw, C., Pagnier, H., Simmelink, H., Van Wees, J.-D., & Verweij, J. (2000). Modelling the hydrocarbon generation and migration in the West Netherlands Basin, the Netherlands. *Netherlands Journal of Geosciences, 79(01)*, 29-44.

Brunton, S. L., & Kutz, J. N. (2017). *Data Driven Science & Engineering.*

Donselaar, M., Groenenberg, R., & Gilding, D. (2015). Reservoir geology and geothermal potential of the Delft Sandstone Member in the West Netherlands Basin. *Paper presented at World Geothermal Congress 2015.* Melbourne, Australia (2015, April).

Giammar, D., Bruant, R., & Peters, C. (2005). Forsterite dissolution and magnesite precipitation at conditions relevant for deep saline aquifer storage and sequestration of carbon dioxide. *Chemical Geology, Volume 217, Issues 3–4*, 257-276.

Karabelas, A. (2002). Scale formation in tubular heat exchangers—research priorities. *International Journal of Thermal Sciences,Volume 41, Issue 7*, 682-692.

Kovács, K., Seres, A., Hartai,É., The H2020 REFLECT project: Deliverable 3.3 – The REFLECT European Fluid Atlas, GFZ German Research Centre for Geosciences, 2023 DOI: https://doi.org/10.48440/gfz.4.8.2023.002

Lassin, A., Laurent, A., Devau, N., Lach, A., Beuvier, T., Gibaud, A., Azaroual, M. (2018). Dynamics of calcium carbonate formation: Geochemical modeling of a two-step mechanism. *Geochimica et Cosmochimica Acta, Volume 240*, 236-254.

Ness, G., Confidimus, F., Sorbie, K., University, H.-W., Al Mesmari, A., & Masalmeh, S. (2021). The Evolution of CaCO3 Scaling Potential in ADNOC Reservoirs Under Water. *Abu Dhabi International Petroleum Exhibition & Conference.* Abu Dhabi, UAE, 15 – 18 November 2021: SPE.

Parkhurst, D. L., & Appelo, C. (2013). *Description of input and examples for PHREEQC Version 3 – a computer program for speciation, batch-reaction, onedimensional transport and inverse geochemical calculations.* U.S. Geological Survey Technical Methods Report, book 6, chapter A43, 497 pp.

Poort, J., de Zwart, H., Wasch, L., & Shoeibi Omrani, P. (2022). *Impact of Geochemical Uncertainties on Fluid Production and Scaling Prediction.*

Ramstad, K., Sandengen, K., & Mitchell, A. (2020). Correlating Calcium Carbonate Scale Risk with Field Experience Data. *Paper presented at the SPE International Oilfield Scale Conference and Exhibition.* Virtual.

Sasaki, M., Sorai, M., Okuyama, Y., & Muraoka, H. (2009). Geochemical features of hot and mineral springs associated with large calcareous deposits in Japan - A potential natural analog study for CO2 underground sequestration. *Japanese Magazine of Mineralogical and Petrological Sciences, Volume 38, Issue 5*, 175 – 197.

Schreiber, S., Lapanje, Ramsak, P., & Breembroek, G. (2016). Operational issues in Geothermal Energy in Europe: Status and Overveiw. *Operational issues in Geothermal Energy in Europe.* Reykjavík.

Todd, M., & Bluemle, M. (2022). Chapter 12 - Formation and mitigation of mineral scaling in geothermal power plants. In Z. Amjad, & K. Demadis, *Water-Formed Deposits* (pp. 269-282). Elsevier.

Wang, F. (2013). *Silicate Mineral Dissolution and Associated Carbonate Precipitation at Conditions Relevant to Geologic Carbon Sequestration.* Washington University, St. Louis, MO: Doctoral Thesis.

Wasch, L. J., Dijkstra, H., & Koenen, M. (2020). Soft-stimulating Injection Procedures to Improve Geothermal Reservoir Performance. *Proceedings World Geothermal Congress 2020 .* Reykjavik, Iceland, April 26 – May 2, 2020.

Wasch, L., Dijkstra, H., Feldbusch, E., Regenspurg, S., Zotzmann, J., Iannotta, J., . . . Shoeibi Omrani, P. (2022). Geothermal performance enhancement with pressure and temperature control – field demonstration and predictive modelling. *European Geothermal Congress.* Berlin, Germany | 17-21 October 2022.

Yeboah, Y., Samuah, S., & Saeed, M. (1993). Prediction of Carbonate and Sulfate Scales in Oilfields. *Paper presented at the Middle East Oil Show.* Bahrain, April 1993: SPE.